12 PVC Extrusions

12.1 Introduction

Rigid PVC extrusions are the basic building blocks of the NOνA detectors. They are the structural elements, the reflectors of scintillation light and the primary containment vessels for liquid scintillator. The mass of PVC used to make the far detector is 4.5 kilotons, which is 30% of the total far detector mass. Extrusions have a cellular structure, with 16 isolated cells per extrusion. Furthermore, there are two types of PVC extrusions differing in thickness but not in outer dimensions: thick-wall extrusions are oriented vertically and bear the weight of the detector (refer to Chapter 17); thin-wall extrusions are oriented horizontally.

All far detector extrusions are 15.494 m long, Extrusions destined for the near detector are 2.63 m long (horizontal extrusions) and 3.94 m long (vertical extrusions) Detector modules are made by joining two PVC extrusions at the sides, as described in Chapter 13. An example of two prototype 16-cell extrusions, 15.5 m long, placed side-by-side, is shown in Fig. 12.1.

This chapter is organized in the following way: After stating the technical design criteria, we present details of the production of PVC extrusions, including the PVC resin composition. Quality control methods are described and dimensional measurements of prototype extrusions are presented. Reflective properties of NOνA PVC and the relationship to light yield are discussed in the next section, followed by a detailed description of the mechanical properties of NOνA PVC, which includes a variety of tests and models used to predict creep in PVC. Shipping and handling techniques are outlined next, followed by a summary of the changes in design since the CDR and the work remaining to complete the PVC Extrusion Design.

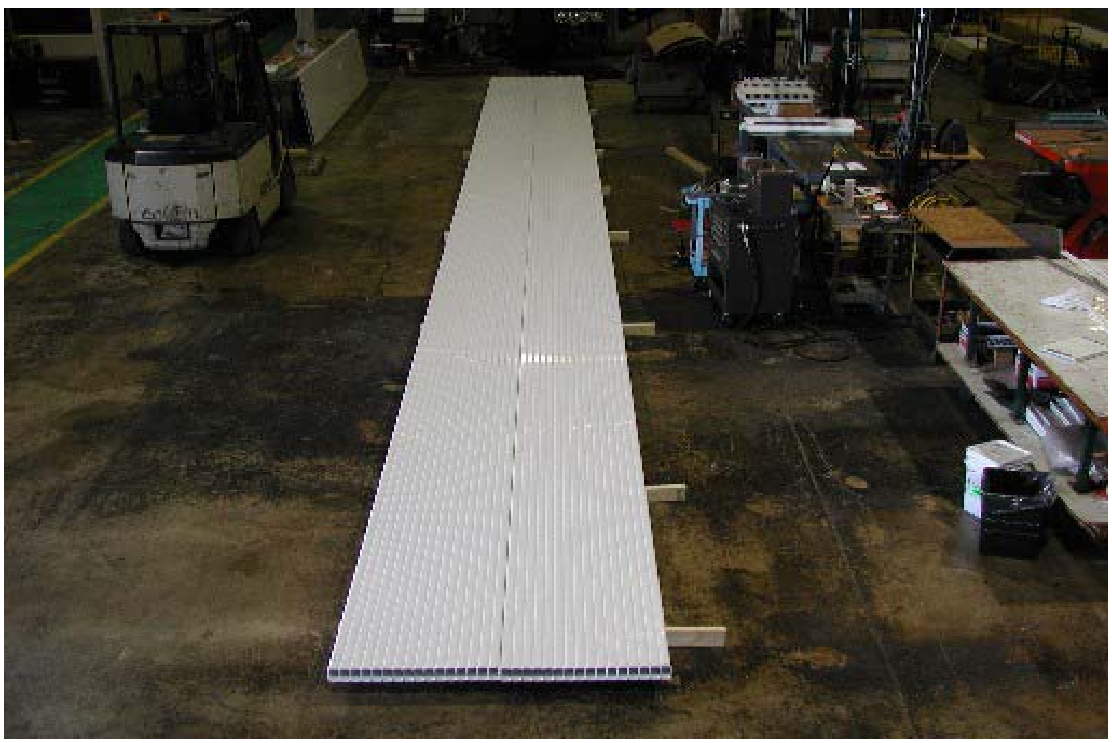

Fig. 12.1: Two 53 foot NOνA prototype PVC extrusions from an early R&D production illustrate the straightness of the extruding process. These 16 cell extrusions are not attached to each other.

12.2 Technical Design Criteria

The major technical design criteria for NOνA PVC extrusions are: (1) they must be sufficiently reflective to produce the required light yield, (2) they must be sufficiently strong to form a self-supporting NOνA detector structure, filled with liquid scintillator, over the lifetime of the experiment and (3) their shape must be within the specified tolerances for assembly of modules and detector blocks.

12.2.1 Light Yield and Reflectivity

NOνA readout electronics requires, at minimum, a 20 photoelectron signal in response to minimum ionizing radiation at the far-end of a 15.5 m NOνA cell as discussed in Chapter 6. The signal strength is due to the APD quantum efficiency and the light yield in response to ionizing radiation. The light yield, in turn, is due to a combination of the PVC reflectivity, the scintillator and wavelength-shifting fiber responses. Because the spectral shape of scintillation light is broad, NOνA PVC material must be highly reflective over a range of wavelengths matching the product of the scintillator emission spectrum and the WLS absorption spectrum.

NOνA PVC is designed to be highly reflective by adding substantially more titanium dioxide (TiO_2) to the PVC resin than is normally used in commercial applications. This can yield reflectivity values as high as 92% at 430 nm, near the peak of the scintillator emission spectrum. However, in order for any PVC compound to be extruded, a number of processing ingredients must be added to the mix. Great care must be taken to ensure that these ingredients have a negligible effect on the reflectivity of the extruded material. Reflectivity and light yield of NOνA rigid PVC is discussed in more detail in section 12.5.

TiO_2 is available commercially in two crystalline types: rutile and anatase. Rutile is generally used throughout the PVC industry but anatase is not. PVC with anatase is said to be more difficult to extrude and the extrusions don't hold up well outdoors, exposed to sunshine and rain. However, anatase offers an advantage to NOνA because it extends the high reflectivity of PVC by ~30 nm to wavelengths below 400 nm. This extended range is enough to overlap most of the short-wavelength tail of the scintillator emission spectrum. Direct comparisons of NOνA extruded PVC detector cells, filled with liquid scintillator and instrumented with WLS fibers, showed 15% more light yield for extrusions made with anatase as compared to extrusions made with rutile.

Since the NOνA experiment will not be subjected to harsh outdoor conditions, we have decided to use the anatase form of TiO_2. Mechanical strength tests and light yield tests show no adverse effects due to the use of anatase when exposed to liquid scintillator. Therefore the technical requirement for reflectivity assumes the use of anatase as the reflective ingredient in the PVC mixture. More details are presented in section 12.3.1.

The NOνA technical design requirement for reflectivity within all of the 16 cells in an extrusion is based on light yield tests described in section 12.5.2. It is required that the reflectivity is a monotonically increasing function of the wavelength (refer to Fig. 12.21) and that the value of the reflectivity is at least 78% at a wavelength of 400 nm and at least 90% at a wavelength of 430 nm.

12.2.2 Strength

The second technical criterion concerns the material strength of PVC. Because the extrusions are used as the structural members in the NOνA design (see Chapter 17), NOνA PVC must meet minimum strength requirements determined by the structural demands. Strength requirements are normally defined by the material's yield and ultimate stress. In the case of PVC as used in this structure, the dominant mechanical property is that of creep. In order to minimize creep, the stresses are kept below 700 psi. This is well below the yield and ultimate stresses of

PVC which are typically > 4000psi and > 6000 psi, respectively. Additionally the PVC must have sufficient impact strength and exposure to the liquid scintillator should not lower any of these values significantly. Strength of PVC is discussed at length in Section 12.6.

For structural reasons, extrusions come in two types: one with 3 .3 mm exterior walls and 2.3 mm interior webs for horizontal cells, and a thicker version with 4.8 mm exterior walls and 3.3 mm interior webs for the vertical cells. This difference is required because the horizontal extrusions filled with scintillator are supported by vertical extrusions that transmit the load to the floor (See Chapter 17). The exterior sizes of horizontal and vertical extrusion are identical for assembly purposes. Therefore the interior cells sizes of vertical extrusions are slightly smaller than the horizontal interior cell sizes.

The NOνA technical design for PVC strength requires a tensile strength of 6,000 psi and a creep modulus (after 20 years) of at least 75,000 psi. The creep modulus characterizes the "plastic" nature of the PVC and is discussed in Section 12.6. The strength properties of rigid PVC are not strongly influenced by our optimization of the PVC formulation to attain high reflectivity.

12.2.3 Shape

The third technical design criterion requires that PVC shape must be within specified tolerances to facilitate assembly of modules and detector. This puts constraints on thickness, flatness and straightness of the extrusion's outside edges (bond two 16-cell extrusions to make one 32-cell module), the extrusion's profile (manifold and bottom plate must mate to two extrusions properly), and the extrusion's flatness (upper and lower extrusion surfaces must attach in the process of block assembly).

The shape of vertical and horizontal extrusions must meet the design profiles, within tolerances stated, as shown in the engineering drawings on the next two pages. The dimensions for horizontal and vertical extrusions are shown below in Figures 12.2 and 12.3. Extrusion thickness is determined by the structural considerations presented in Ch. 17. The outside walls of horizontal extrusions are 3.3 (+ 0.7/-0.3) mm thick and the inner walls, called webs, are 2.3 (+0.7/- 0.3) mm thick. The outside wall of vertical extrusions outside walls are 4.8 (+0.7/-0 .3) mm thick and the webs are 3.3 (+07/- 0.3) mm thick.

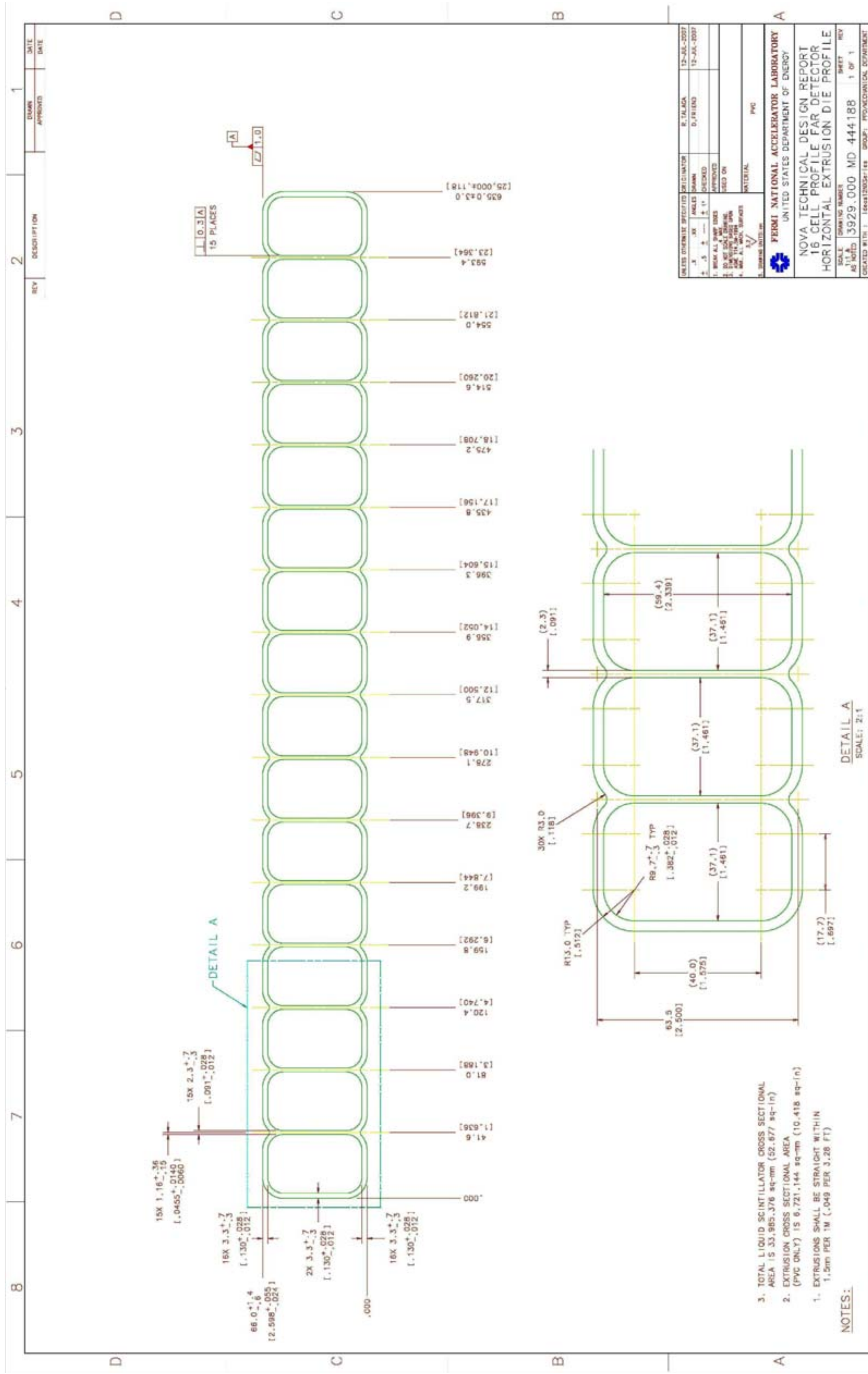

Fig. 12.2: Drawing of the NOνA thin-walled extrusion for horizontal modules.

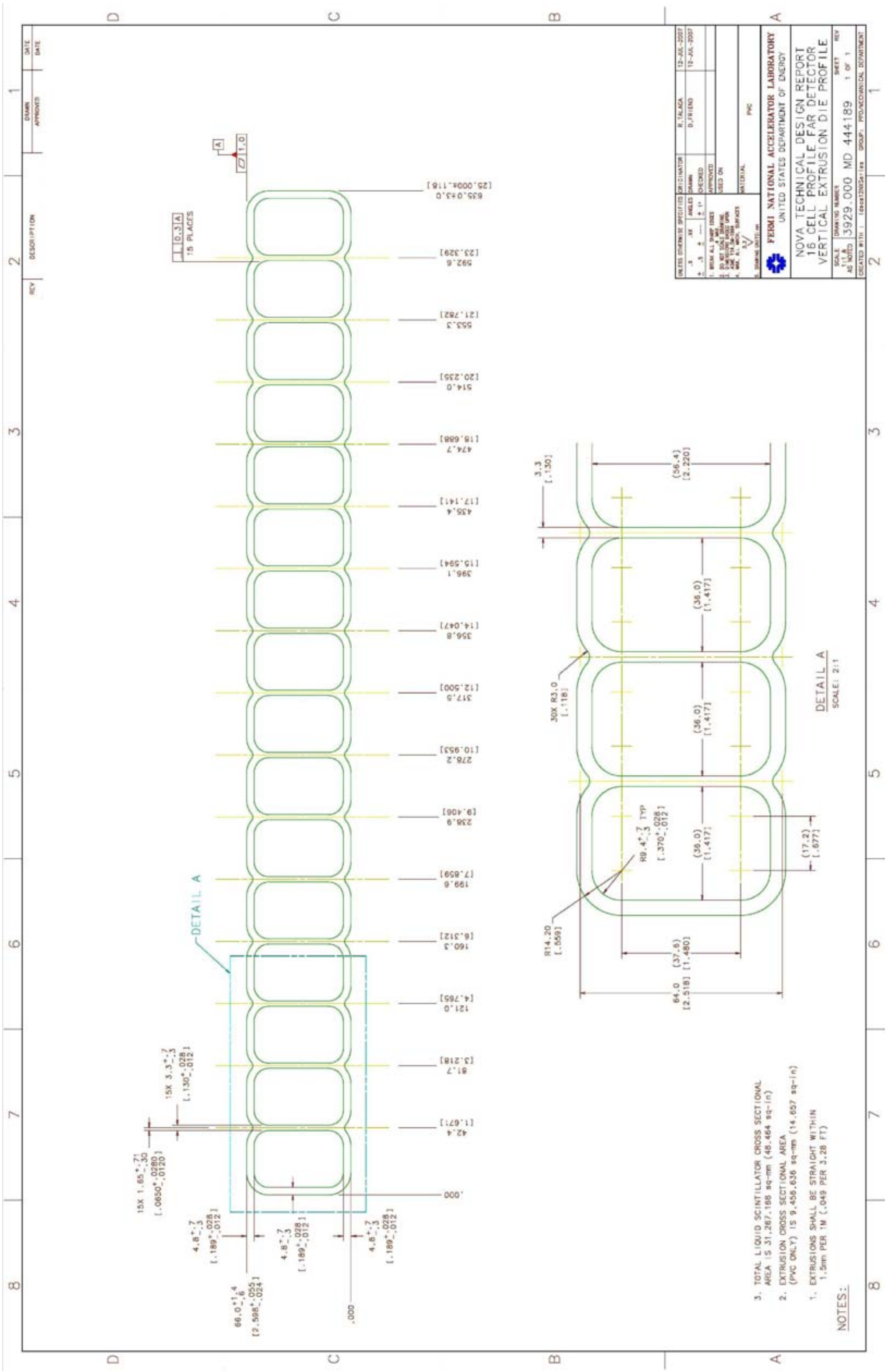

Fig. 12.3: Drawing of the NOνA thick-walled extrusion for vertical modules.

12.3 PVC Resin and the Extruding Process

Production of extrusions is a two-step process. The first step is to mix PVC polymer with titanium dioxide and a number of processing aids to produce a NOνA specific resin called N-27. This is performed by a commercial compounding firm. The second step is to produce rigid PVC extrusions at an extruding company. There, the resin (in powder form) is inserted into an extruding machine where it is melted and pushed through a NOνA-designed die. After exiting the die, extruded PVC enters water-cooled sizing tools that helps maintain the shape (by vacuum suction) as the extrusion is cooled. After the extrusion exits the sizing tools it enters water tanks to remove residual heat, ensuring the extrusion to be at room temperature upon exit.
After the extruded PVC is cut to length it is labeled, measured and placed in one of four sorting stacks, depending on the height of the extruded profile (refer to section 12.4.2). Once a stack of extrusions is full, it is packaged for shipment.

12.3.1 PVC Resin Composition

Selection of the quantity and type of TiO_2, the processing aids and the PVC polymer was made after almost two years of R&D, which included consultation with James Summers, an expert on PVC production, and close interaction with two commercial compounding companies, an independent plastics laboratory, and two commercial extruding companies and their production staffs. The ultimate goal of the R&D was to produce a formulation that, when extruded, produces PVC extrusions with excellent reflectivity, mechanical strength and geometrical shape.

PVC will not extrude without addition of processing aids to the polymer, which typically number anywhere between 5 and 10 ingredients. In the extruding process, the PVC resin is subjected to pressures up to 4,000 psi and temperatures of nearly 400 degrees F for a significant period of time. The processing aids (stabilizers and lubricants) are added to the PVC polymer and the TiO_2 to keep molten resin flowing through the die without sticking, burning or otherwise decomposing. Care must be taken to ensure that processing aids do not have adverse effects on the reflectivity or strength of the extruded product.

The reflectivity requirement of NOνA posed a challenge in the selection of specific processing aids, the type of PVC polymer and the type and brand of TiO_2. Extensive laboratory R&D was performed on over two dozen formulations with particular attention paid to reflectivity; those with satisfactory results were extruded and their extrudability, mechanical properties and reflectivity were evaluated.

In addition to selecting the resin formulation, the mixing method was also optimized. This is the order in which ingredients are mixed with the polymer, the length of time and the temperature of the mixture.

Commercially available PVC resins are proprietary and their reflectivity properties are not optimized for NOνA. In order to control all of the ingredients and, in some cases, the brand names of ingredients, we have developed a resin formulation that meets NOνA requirements for reflectivity, strength and extrudability. This resin is called NOνA-27, or N-27. The ingredients in the N-27 resin are PVC, tin stabilizer, TiO_2, calcium stearate, paraffin wax, oxidized polyethylene and glycerol monostearate. They are listed in Table 12.1, along with the commercial brand names and the relative proportion by weight: parts per hundred. The PVC and other ingredients were specifically selected to optimize reflectivity. The net result is a rigid PVC compound with 14.7% anatase TiO_2 by weight.

N-27 PVC Resin			
Ingredient	**Commercial Brand Name**	**Parts per Hundred**	**per cent**
PVC	Shintech SE950EG (high reflectivity)	**100**	**77.5%**
Tin stabilizer	Rohm & Haas Advastab TM-181 20% monomethyl tin	**2.5**	**1.9%**
Titanium dioxide anatase	Kronos 1000 anatase titanium dioxide	19	**14.7%**
Calcium stearate	Ferro 15F calcium stearate	**0.8**	**0.6%**
Paraffin wax	Ferro 165 paraffin wax	**1.1**	**0.9%**
Oxidized polyethylene	Ferro Petrac 215 oxidized polyethylene	**0.2**	**0.2%**
Glycerol monostearate	Rohm & Haas F1005 glycerol monostearate	**0.3**	**0.2%**
Acrylic impact modifier	Arkema Durastrength 200 Acrylic impact modifier	**4**	**3.1%**
Processing aid	Rohm & Haas Paraloid K120N processing aid	**1**	**0.8%**
	Total	**129**	**100%**

Table 12.1: Composition of N-27 rigid PVC compound.

Selection of the N-27 formulation was made after testing a number of PVC resins, both proprietary and those developed by NOνA. The criteria for selection are: (1) there should be no significant build-up or sticking of the resin to the NOνA 16-cell die over a period of at least two days of continuous production, (2) the resin produces a complete extrusion with proper welding of all interior webs to the outside walls and (3) the extrusion produces the highest light yield in response to ionizing radiation when it is filled with liquid scintillator and equipped with a fiber (as explained in section 12.5.2). N-27 met these requirements and had the fewest additives of any of the candidates.

N-27 resin produces an extrusion with density equal to 1.49 gm/cc. Given this density and the nominal profile dimensions shown in Figs. 12.2 and 12.3, the thin-wall horizontal extrusions weigh 10.0 kg/m and the thick-wall vertical extrusions weigh 14.1 kg/m.

12.3.2 *Extruding the PVC Resin*

The extruding process utilizes a number of custom-made tools and commercial components arranged in a sequential order. This “extrusion line” begins with the extruding machine, a high-capacity twin-screw extruder. This is followed by a die, sizing tools, cooling tanks, a “puller” and a traveling saw. The die, sizing tools and cooling tanks are custom-made for NOνA. The extruder, puller and traveling saw are commercial products, as is the movable table that supports the sizing tool and cooling tank. A photo of the extruding line used for production of NOνA prototype extrusions is shown in Figure 12.4. Additional photos of the individual components in the extruding line are shown in Figures 12.5 through 12.9.

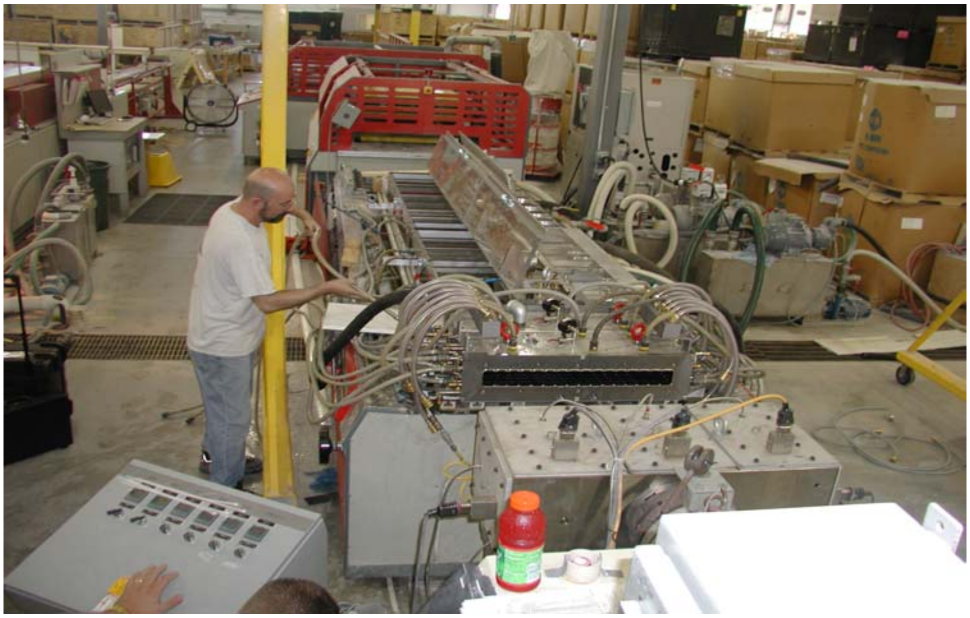

Fig. 12.4: Extruding line for NOνA prototype production. A partial view of the extruding machine is at the bottom right of the picture with the prototype 16-cell die just beyond it. The wide opening beyond the die is the entrance to the vacuum sizing tool, which is followed by the water cooling tank. The smaller red object downstream of the cooling tank houses the extrusion puller and the larger red object at the very top of the picture houses the cutting station.

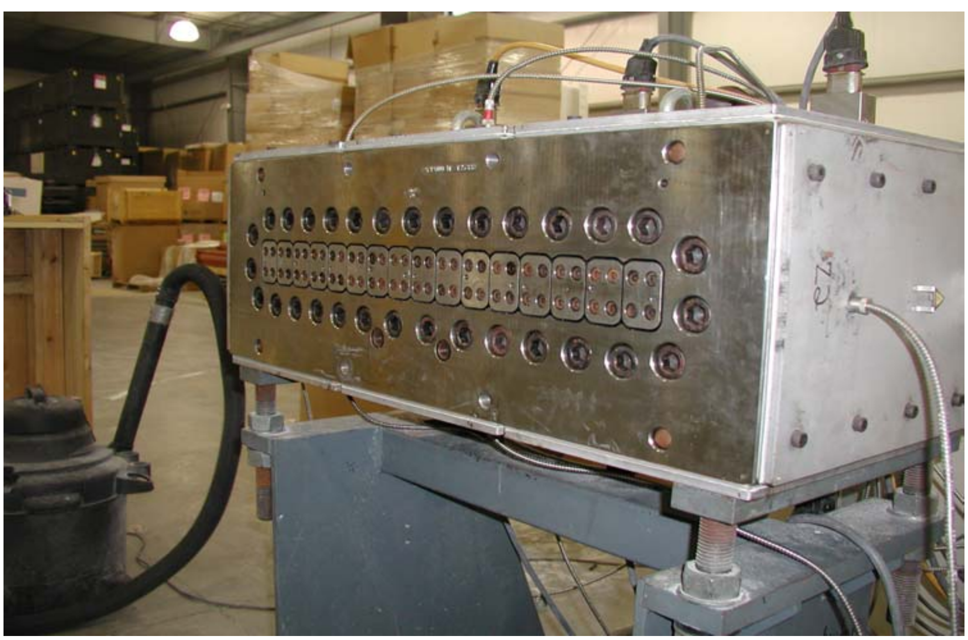

Fig. 12.5: The custom NOνA prototype 16-cell die. PVC resin moves right to left and exits the die through the scalloped profile shown in this view.

Fig. 12.6: The custom NOνA vacuum sizing tool. During production, this tool is in close proximity to the exit face of the die. As the molten PVC exits the die the water-cooled sizing tool keeps extrusion shape from collapsing by sucking the outside walls of the extrusion against the walls of the sizing tool .

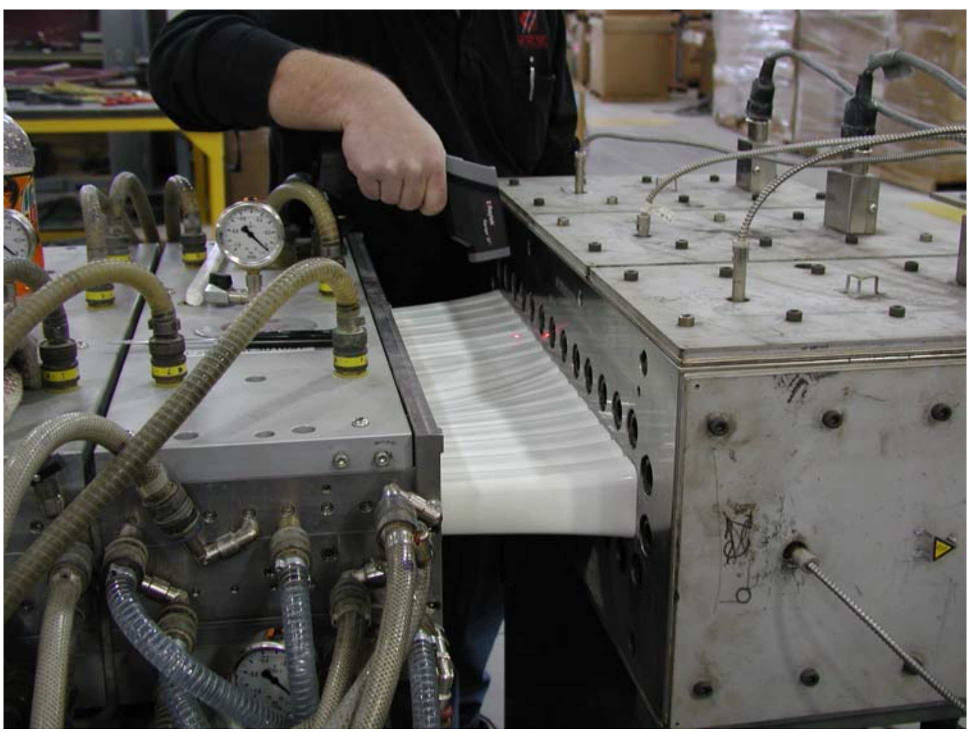

Fig. 12.7: PVC exits the die (on the right) and moves toward the vacuum sizing tool at startup. PVC melt temperature is measured just outside the die. After this inspection, the sizing tool is moved up against the die and vacuum suction is initiated.

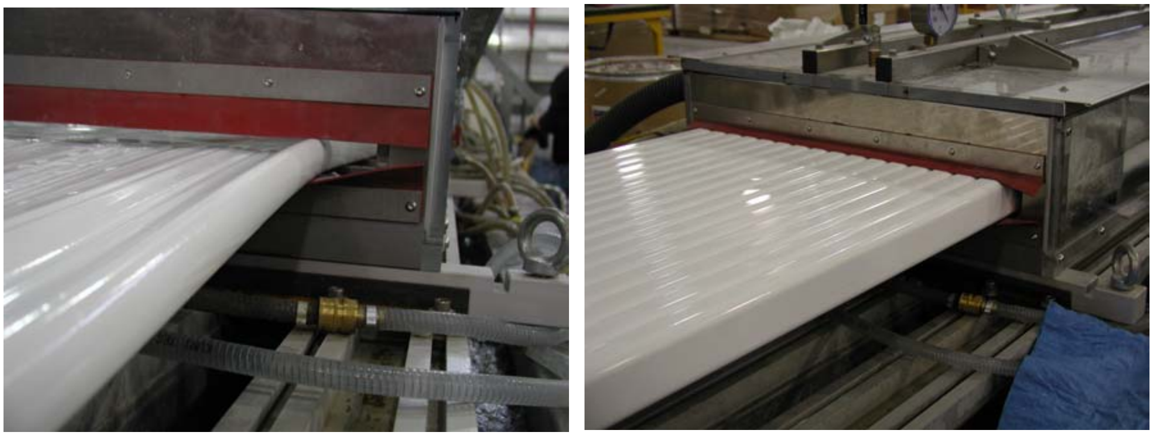

Fig. 12.8: PVC exits the water cooling tank. The photo on the left shows PVC at startup, before vacuum is applied in the sizing tool. The photo on the right shows the effect of the vacuum sizing.

Fig. 12.9: A prototype extrusion exits the cutting station. Note the uniform cell dimensions and wall thicknesses.

The Extruding Process requires tuning a large number of operating parameters to produce an acceptable extrusion. Parameters include temperatures (four temperature zones in the extruding machine barrel, 8 temperature zones in the die and the temperature of the screws), the PVC resin input rate, the speed of the puller, the strength of the vacuum in the sizing tool, the strength of vacuum in the water cooling tanks and the size of the separation gap between the die and the sizing, among others. Fine adjustment of the vacuum is critical because of the resistance due to friction may overcome the strength of the puller. Additional components can be inserted into the extruder to affect pressures and temperatures. One example is the "breaker plate" outfitted with fine-mesh screen(s). The extruding company's personnel adjust these parameters, often with the aid of the die maker, to produce a product that meets NOνA size and shape specifications.

12.3.3 Prototype Extrusions

The NOνA prototype die, sizing tools and water cooling tanks were ordered in December 2005 for use in resin development and prototype extrusion production. The die makes a 16-cell PVC extrusion that is 30 mm wider than what is called for in the NOνA technical design (refer to Figs 12.2 and 12.3). The prototype die accommodates exchangeable "inserts" to produce either thin-walled prototype extrusions for horizontal modules or thick-walled prototype extrusions for vertical modules. Since the external dimension of thin-walled and thick-walled prototype extrusions are identical, the vacuum sizing and water cooling tank accommodate either type of extrusion.

After a period of testing a number of potential PVC resins designed to produce highly reflective extrusions, N-27 resin was selected for making the majority of prototype extrusions. The resin tests were performed with the thin-wall extrusion die. Once N-27 was selected, it was tested with the thick-wall die, which has a capacity for resin 41% larger than the thin-wall die. Because the extruding machine operates near its maximum output, resin moves slower through the thick-wall die and there was concern that the longer residence time may degrade the resin. Fortunately this was shown not to be the case and the quality of thick-wall extrusions was not degraded due to the longer residence time.

The Extruding Process is defined by the settings of a number of operating controls, as mentioned above. Extruding output is approximately 550 pounds per hour. The Process was tuned for N-27 resin to produce acceptable extrusions under a stable set of operating parameters. The die components were machined, based on feedback from initial test extrusions, to produce prototype extrusion profiles that satisfied the dimensional specifications.

Prototype extrusions have been produced with the NOνA die using the thin-wall and thick-wall die inserts. These extrusions are used in several applications discussed in Chapters 5 and 17, including the Integration Prototype Near Detector (IPND), the Full Scale Assembly Prototype (FSAP), the Full-Height Engineering Prototype (FHEP), and test structures for structural prototypes and for material properties.

12.3.4 16-Cell Extrusions

Although NOνA modules are 32-cells wide, the prototype die and tooling are designed to produce 16-cell extrusions to keep R&D costs affordable. There are at least three factors that raise the cost significantly in making 32-cell extrusions. First, the size of such a wide die becomes a factor due to flow requirements and degradation of PVC resin due to the residence time. We are not aware of any PVC dies (except for simple sheet dies) of such width (1.27 m) and complexity in use anywhere in the world. Second, extruding manufacturers are not set up to produce PVC extrusions wider then 1 meter (except for sheet PVC). Third, the cost of a 32 cell die would have been more than double the cost of the prototype die, adding to the R&D budget.

Experience with the NOνA 16-cell prototype die showed that although a PVC resin can be extruded in a small die it may still fail (burned resin, webs not knitted, etc.) in the larger die. After conducting a variety of resin tests over the past year, it was decided to forego the additional expense and risk of making a single extrusion 1.27 m wide (32 cells). Instead, 16-cell extrusions will be made and 32-cell modules will be made by bonding two 16-cell extrusions. This is discussed in Chapter 13.

12.4 Extrusion Production

In total, approximately 4,500 metric tons of rigid PVC will be produced for the NOνA detectors over a two year time span. Before the start of extrusion production, the new thick-wall and thin-wall dies must be fabricated, tested and tuned, if needed to produce acceptable extrusions. After the extrusions are deemed to be acceptable, the next step is to make pre-production extrusions. Here, the purpose is to validate the long-term stability of the Extruding Process. Some of the pre-production extrusions will be provided to the NOνA Collaboration for various uses. Most of the extrusions will be saved and used as bridge material for shipping stacks of production extrusions (refer to section 12.7).

Extrusion production will begin after the pre-production validation is complete. Production will be on a 5 day per week, 24 hour per day basis with weekly down time for maintenance. A single extruding machine with a nominal throughput of 950 pounds per hour will be used to produce thin-wall and thick-wall extrusions on an alternating basis of approximately 2 weeks for thin-wall and 3 weeks for thick-wall extrusions. Details of the production are provided in the next section.

12.4.1 Die tuning and Pre-Production

Initially, the die flow is tested by the die manufacturer (sub-contracted by the extruding firm). If the flow is not uniform, the die is taken apart and machined to produce the desired flow pattern. Flow is a strong function of the resin formulation and compounding procedures as well as the extruding process parameters. Care will be taken in the resin compounding process to ensure that batch-to-batch variations will be minimal.

After it has been verified that flow of the specified resin is uniform, the die is placed in the extruding line and tested again. If the extrusion does not meet NOνA size and shape specifications the die is taken apart and machined to modify the flow as required. Once die tuning is completed and the process parameters are determined, pre-production can begin.

As noted above, pre-production will validate the long term stability of the Extruding Process by extruding continuously for at least 32 hours. It is very important that the operating parameters and resin quality allow continuous production without requiring down time to stop the run and clean the die. In prototype tests extrusions have been produced at rates between 500 and 600 pounds per hour. The size and weight of NOνA PVC extrusions, especially the thick-wall extrusions for vertical detector modules, require an extruder with a higher throughput. The NOνA PVC production plan calls for a higher-capacity extruding machine allowing production at a rate of 950 lbs. per hour.

The higher-capacity extruder benefits NOνA in two ways. First, it will decrease the residence time of resin in the die, reducing the time the molten PVC is exposed to high temperatures and thereby reducing the risk of the PVC sticking and burning in the die after a week-long continuous production. Second, it will allow the use of a single extruding machine to produce extrusions for horizontal (thin-wall) and vertical (thick wall) modules to meet the NOνA funding profile. It also allows the option to use two extruding lines: the higher capacity machine for producing thick-walled extrusions and the existing machine for producing thin-walled extrusions.

12.4.2 Extrusion Production

Die fabrication and tuning is expected to take approximately one year. Production of extrusions for the first two blocks will take place gradually over several months, to fit the integrated NOνA production and funding schedule. This period will also allow time to fine-tune the dies, to make adjustments to the extruding process, and to perform detailed quality assurance tests.

After this startup period, extrusion production will proceed continuously, with normal breaks for maintenance. The 744 extrusions for each 31 plane detector block will take approximately 15 to 16 work days to produce. It is more efficient to produce extrusions of one type (thin-wall, for example) for two blocks before switching the extruding line over to produce extrusions of the other type. The plan is to produce thin-wall horizontal extrusions for two blocks of the far detector and then switch over to produce thick-wall extrusions for those blocks. Typically, a switch over takes at least one shift to accomplish. This production rate is in step with the expected speed of module and detector assembly. Continuous production of all extrusions required for NOvA will take approximately 22 months.

After an extrusion is taken off the extrusion line, it is placed in one of four shipping stacks depending on the extrusions' average height. Nominal height is 66 mm but the dimensional tolerance is liberal: (+1.4 -0.6) mm, In order to optimize bonding of orthogonal detector planes, extrusions are sorted by height to ensure that one plane of modules will have minimal height variation..

12.4.3 Quality Assurance and Quality Control

NOvA extrusions will be produced with a well-defined set of acceptance criteria. Quality assurance begins with a comprehensive Manufacturing Plan, specified by the extruding company in consultation with the NOvA project. This Plan includes a detailed description of the tooling used in the extruding process, adjustment of tooling and manufacturing parameters to produce acceptable parts, establishment of a standard set of machine operation parameters and acceptable deviations and a set quality control measurements of the finished product with prompt feedback to machine operators whenever necessary.

Process variables, such as extruder temperatures, pressures, puller speed, screw speed, screw thrust, sizing-tool vacuum, water flows and other parameters are recorded regularly. A process window for each variable is defined. This process window is the result of prior testing and to assure that acceptable mechanical properties result from consistent process parameters.

12.4.3.1 Measurements at the Extruding Manufacturer

Based on R&D experience with NOvA prototype extrusion production, measurements of every extrusion produced will be made at the extruding company. Objectives and the methods for making the measurements are listed below.

1. Visual Observations
   - Inspect the surface quality of the extrusion for any irregularities
   - Inspect the ends of the extrusion for irregularities, voids or bubbles within the plastic and for the quality of web knitting. Examples of irregularities are shown in Figure 12.10.

Fig. 12.10: Visual inspection detects irregularities in surface texture (chatter marks in photo on left side) and incomplete knitting of the center lower web (photo right side).

2. Weight
   - The net weight of an extrusion is measured via a scale on the lifting fixture (refer to section 12.7) immediately after the extrusion is cut. Data from a prototype production run is shown in Fig. 12.11.

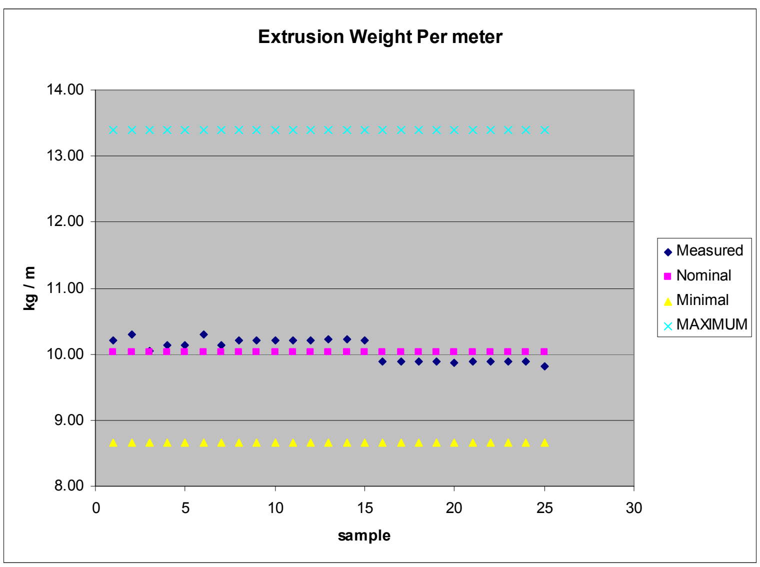

Fig. 12.11 Weight distribution of 25 prototype thin-wall (horizontal) extrusions as a function of sample number, or time. Note that the weight per meter of each sample is close to the nominal value, not near the extreme limits allowed by the tolerance specification.

3. Dimensional measurements of the extrusion's dimensions and log into data base.
   - The thickness of each of the 15 webs
   - The top and bottom cell walls.
   - The extrusion width
   - The extrusion height
   - Deviations from flatness on the top and bottom surfaces. An early prototype of a device to measure flatness deviations is shown in Figure 12.12.

Fig. 12.12: Deviation from flatness of the outer cell dimensions cell is measured by a prototype NOνA QC device.

4. Reflectivity: Confirm extrusion exceeds minimal reflectivity requirement.

- Use portable spectrophotometer to measure reflectivity of outer extruded outer surfaces in the range between 400 and 470 nm.

12.4.3.2 Measurements at Fermilab and ANL

As part of the Production Procedure, a six inch sample extrusions is cut off the production line after production extrusion is made. Approximately 66 samples are collected over a 24 hour period and sent to Fermilab on a daily basis for hydraulic pressure testing. The purpose of these tests is to verify that the junctions of webs and walls throughout the extrusion are strong. Any failure of cell structure indicates poor “knitting” in the extrusion process. The corresponding production extrusions will be flagged and the extruding operator will be alerted.

In order to test batch-to-batch variations of the PVC compound as well as the quality of extrusions, two 18-inch samples are collected twice per shift, for a total of 6 samples in a 24 hour period. These samples will be cut into two 9 inch pieces. One is tested for tensile and reflectivity properties. The other is tested for impact properties.

1. Structural Properties

- Pressure test: Clamp a 6-inch piece sample between two end-seals. The sample is pressurized to 30 psi to confirm web strength. Any obvious cracking or localized excess deflections are due to web failure. Additional fixturing may be needed to allow to varieties of this test so that knit lines in the outer surfaces can also be tested. A prototype device and the result are shown in Fig. 12.13.

Fig. 12.13: Hydraulic test of six-inch PVC extrusion is tested in a prototype machine. The result of this test shows failure (photo on the right) of the web attachment to the lower wall and a failure of the outer wall, as indicated by the black strips lodged in the failed locations.

- Buckling test: Insert a 6-inch extrusion into a fixture and determine how much force it can withstand until the extrusion buckles. A prototype device to test buckling strength and the result are shown in Fig. 12.14.

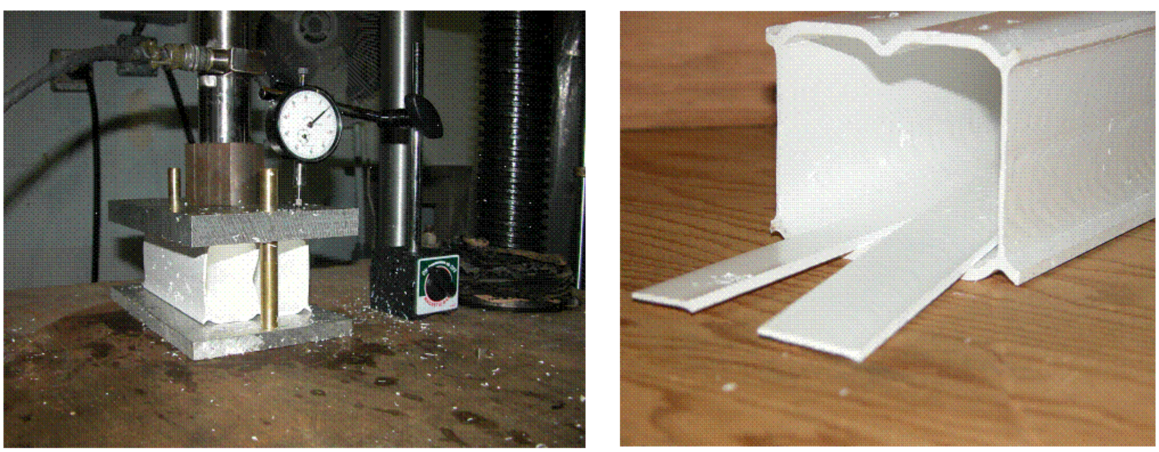

Fig. 12.14: Photograph of a prototype device to test buckling strength of a segment of the PVC extrusion. The photo on the right shows the result of excessive buckling: a failure of the web at its center line (web split in two) and failure of web bonding to the upper and lower walls.

2. Mechanical Properties
   - Impact Resistance . A standard Drop Dart Impact Test is performed on one half of the 18-inch sample. The data is compared to a minimal threshold value and to a historical trend. Fixturing is required for repeatability of a drop dart test, which is dependent upon strike position in cell.
   - Tensile tests will be performed to measure the Young's modulus.

3. Reflectivity properties

- Detailed measurements of reflectivity of the *inner* surfaces of the cells will be made.

12.4.4 Characteristics of Prototype Extrusions

The first cycle of prototype extrusions produced about 20% of those needed for the Integration Prototype Near Detector (IPN). Because IPND extrusions are about one fifth the length of far detector extrusions, they are produced about five times faster than extrusions for the far detector. Because of the rapid production of short extrusions, every fifth IPND extrusion made was measured in detail as it came off the extruding line. Thickness of the upper and lower walls of each cell and the thickness of each of the 15 webs separating the cells were measured with an ultrasound device, cross-checked with digital calipers and recorded. The data for 135 extrusions are presented in histograms below (Figs. 12.15 through 12.17).

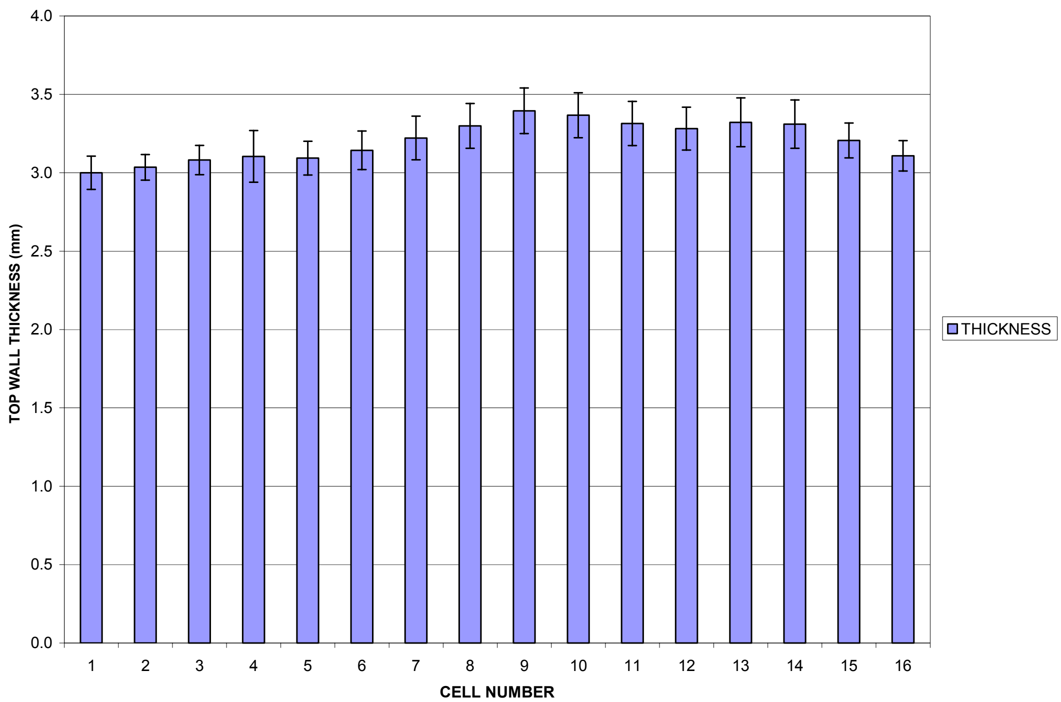

Fig. 12.15: Histogram of top wall thickness as a function of cell number for 135 thin-wall "horizontal" prototype extrusions produced in June 2007. Error bars show the standard deviations.

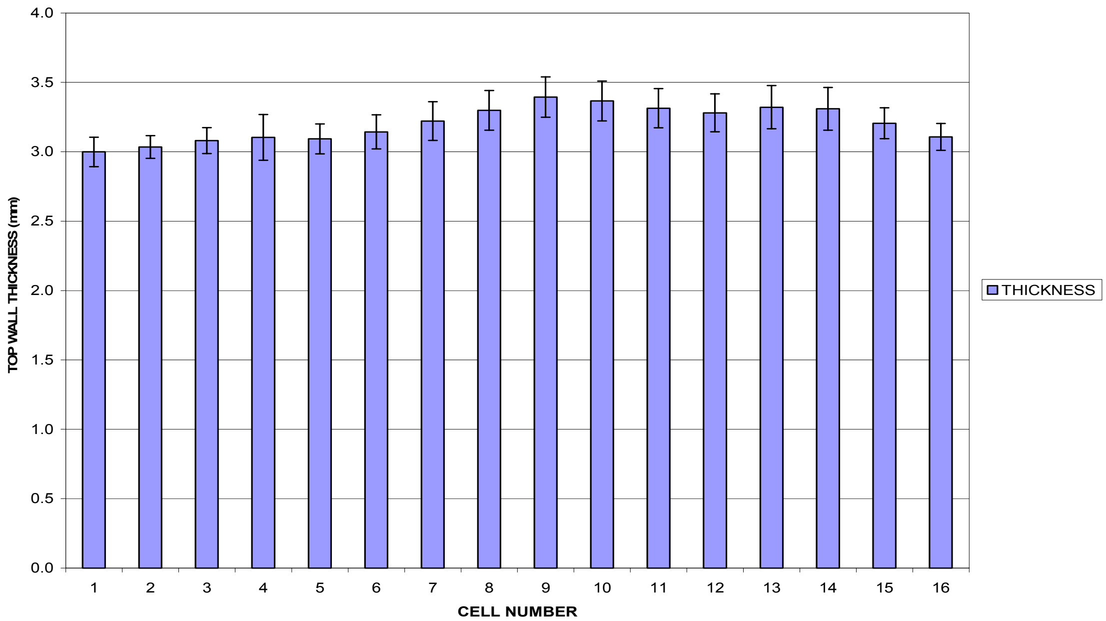

Fig. 12.16: Histogram of bottom wall thickness as a function of cell number for 135 thin-wall “horizontal” prototype extrusions produced in June 2007. Error bars show the standard deviations.

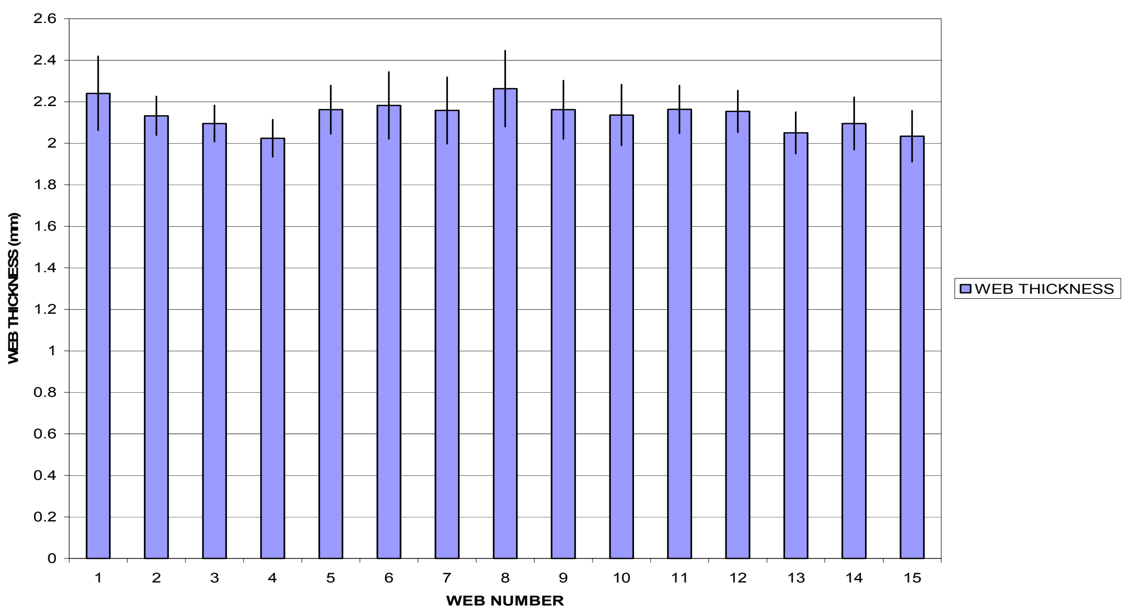

Fig. 12.17: Histogram of web thickness as a function of cell number for 135 thin-wall “horizontal” prototype extrusions produced in June 2007. Error bars show the standard deviations.

Samples also have been measured for flatness; departures from flatness for the top and bottom outer walls of each cell have been recorded and plotted below in Fig. 12.18. Twenty-six 2-foot-long samples were taken over regular intervals during the week-long prototype production run. The average departure from flatness as a function of cell number is shown in Fig. 12.18a and the standard deviations are shown in Fig. 12.18b.

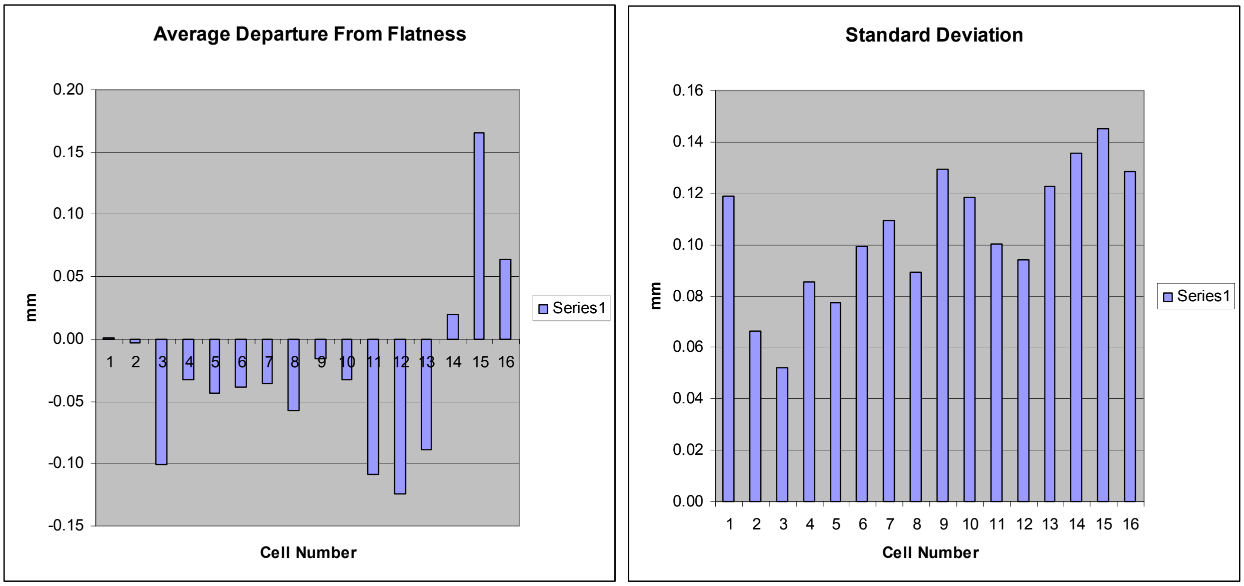

Fig. 12.18: Average departure from flatness (mm) of the top outside surfaces of each cell, shown in the figure on the left (a) and standard deviation is shown in the figure on the right (b).

Weight of extrusions is another quality control check. Twenty five IPND-length (110 inches long) horizontal extrusions made consecutively were weighed; the weight per meter is displayed in Fig. 12.11 as a function of consecutive extrusion number (time). Also plotted are the calculated weight per meter for nominal dimensions, for the maximum allowed dimensions and the minimal allowed dimensions. The data fall within ~2% of the nominal calculated weights indicating that the actual mass of PVC in the detector will be close to the calculated mass.

12.4.5 Prototype Extrusion Reflectivity Measurements

The reflectivity of test extrusions made with N-27 PVC has been measured for a series of 23 consecutively-produced IPND-length extrusions with a portable hand-held spectrophotometer. The reflectivity was measured at three locations along a constant length of the extrusion and averaged. This is one “reflectivity measurement”. Each extrusion had three reflectivity measurements taken along its length: two feet from the near end, at the center and 2 feet from the far end. This resulted in a uniform sampling along 210 feet of extruded PVC. Histograms of the reflectivity at 400 and 410 nm are shown in Figure 12.19.

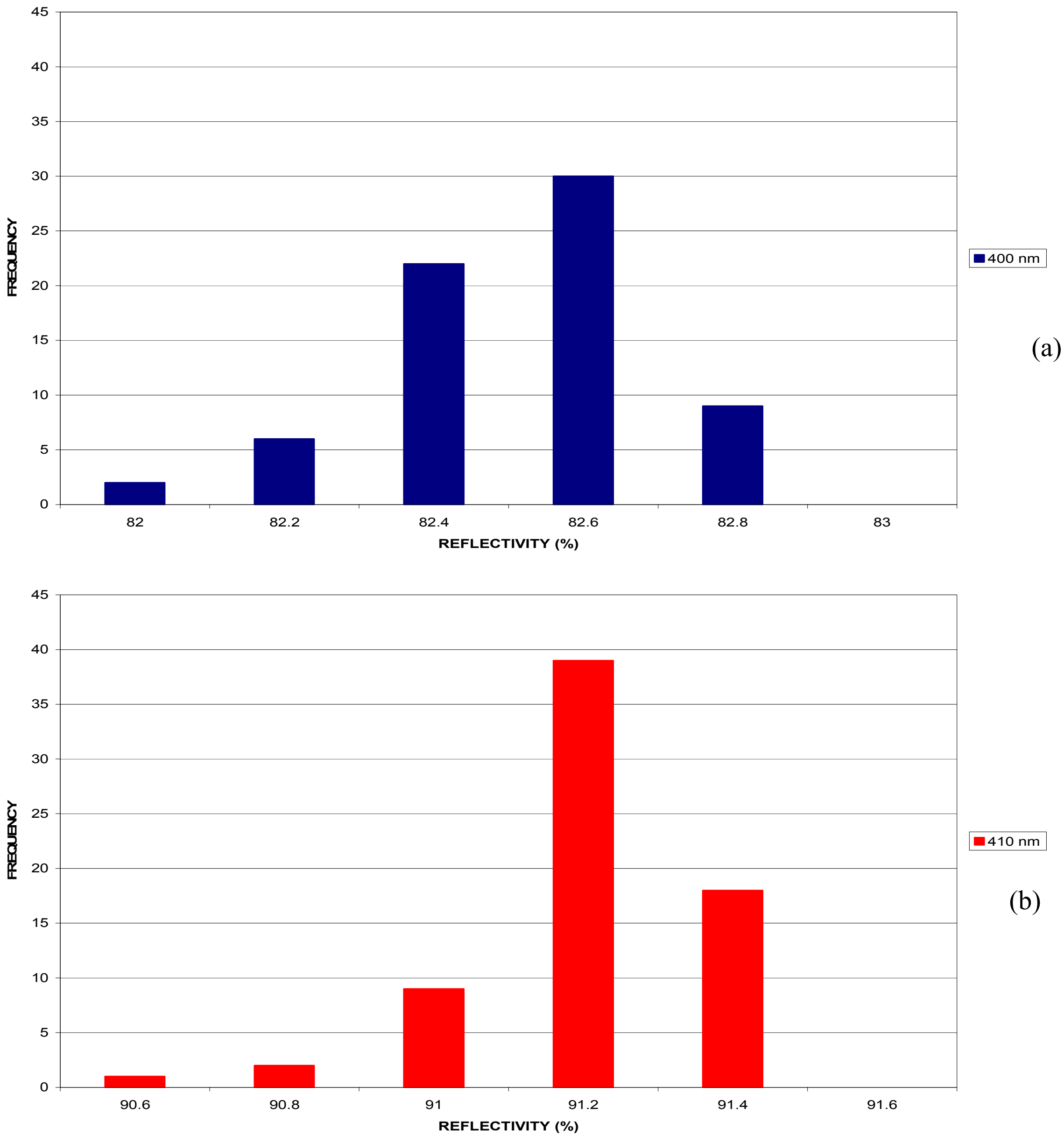

Fig. 12.19: Histograms of the reflectivity of N-27 210 foot sample at 400 nm (a) and 410 nm (b)

The data show the reflectivity of extruded N-27 is constant, to a good approximation, over a length of 210 feet. This result is especially impressive for wavelengths of 400 nm and 410 nm, where the reflectivity changes steeply (refer to Figure 12.21). The data are also plotted in Figure 12.20 in increments of approximately 3 feet along the 210 feet of extrusions.

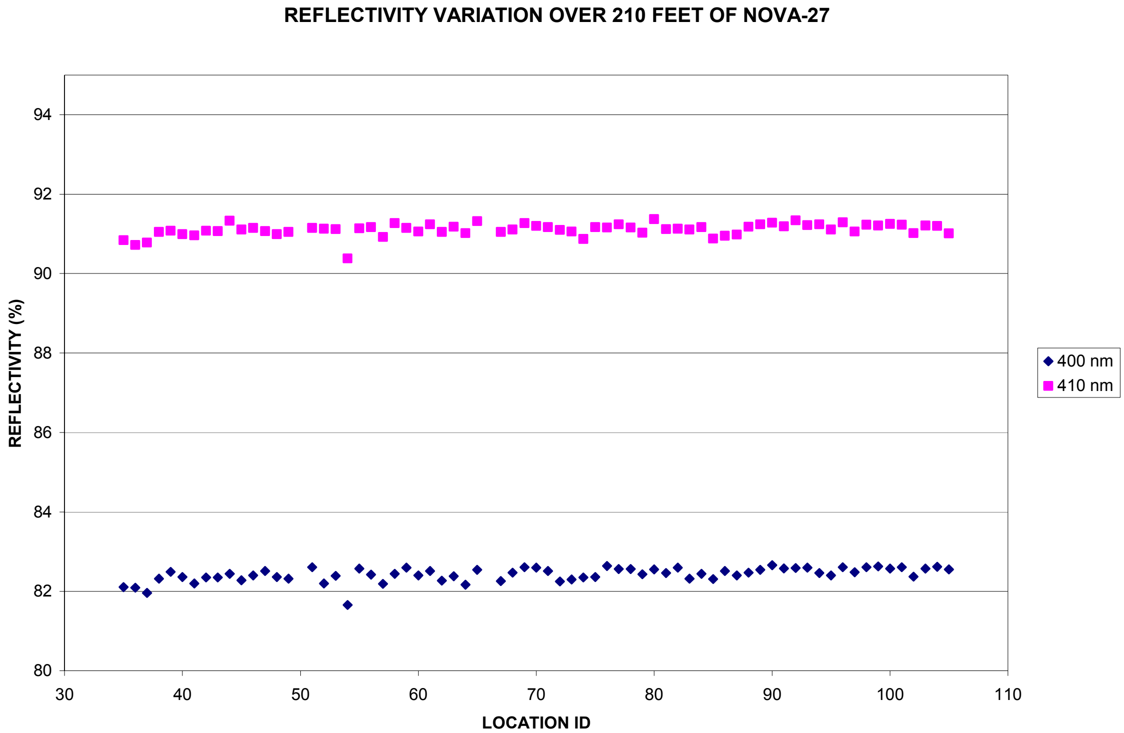

Fig. 12.20: Reflectivity at 400 nm (blue diamonds) and 410 nm (purple squares) taken at uniform intervals over 210 feet of extrusions. The horizontal lines indicate the level of constancy of reflectivity as a function of extrusion production time. Location ID refers to one of 69 samples taken by the spectrophotomer in increments of approximately 3 feet throughout the 210 feet sampled.

12.5 NOνA PVC Reflectivity and Light Yield

NOνA rigid PVC extrusions have been designed to be highly reflective over the spectral output of liquid scintillator to maximize the amount of light captured in WLS fibers. The spectral distribution of scintillator light and the reflectivity of N-27 PVC are shown in Figure 12.17. Reflectivity is mostly due to diffuse reflection which is proportional to the cosine of the angle normal to the surface of the PVC (Lambert's Law). Therefore the primary intensity of reflected light is normal to the surface. Diffuse reflection is due to the titanium dioxide particles in the PVC and the light can scatter off particles that are relatively deep in the material. Titanium dioxide is the best scattering compound because of its high index of refraction (2.73), and blue light is more strongly scattered off particles in the range 0.15 – 0.20 microns [1] .

12.5.1 Reflectivity

The best reflectivity characteristics of extruded PVC are those of N-27, with 15% anatase titanium dioxide. By comparison, reflectivity of PVC with rutile titanium dioxide is comparable at wavelengths of 430 nm and higher, but the anatase titanium dioxide extends the high reflectivity region by approximately 20 nm toward the shorter wavelengths, as shown in Figure12.21.

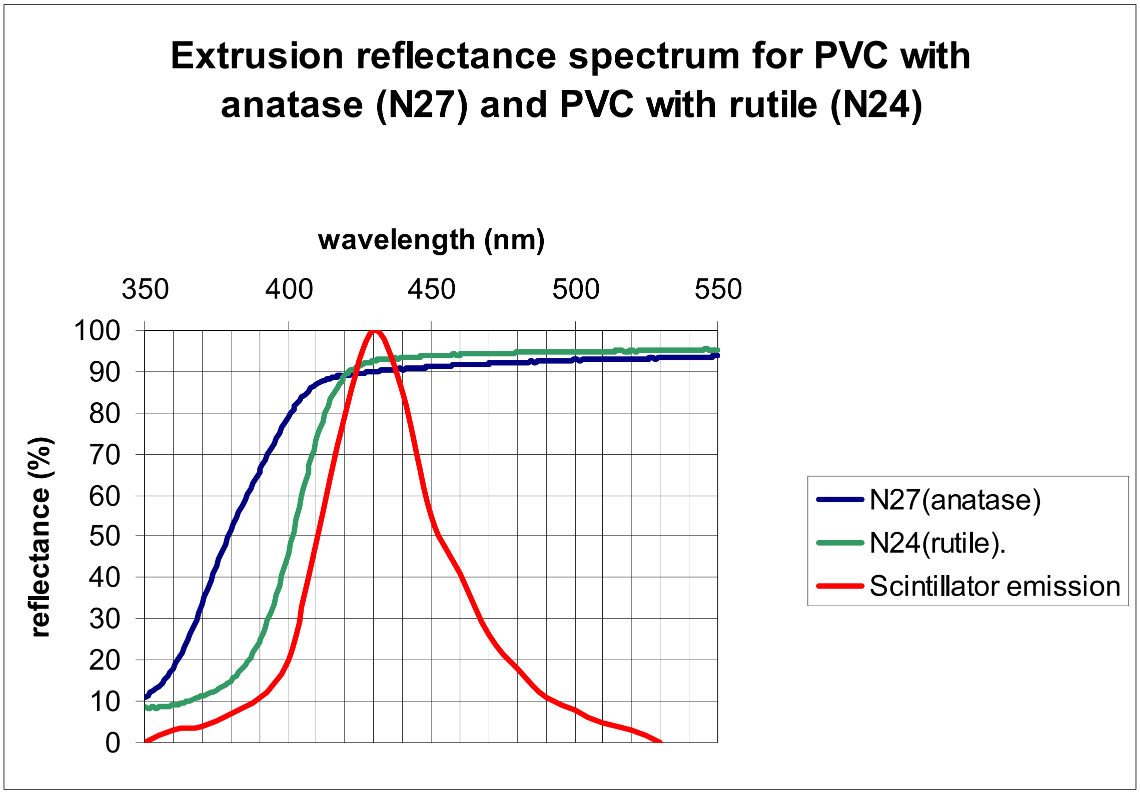

Fig.12.21: Emission spectrum of NOvA Scintillator (red) and the reflectivity spectra of N-27 (blue) and N-24 (green) plotted as a function of wavelength. Note the greater reflectivity at shorter wavelengths due to anatase titanium dioxide in N-27.

Analytic calculations [2] and a Monte Carlo simulation [3] of reflection including diffuse and specular components indicate that light captured by a wavelength shifting fiber is reflected about eight times within the NOvA cell before capture. Eight reflections is the mean of a distribution with very long tails, and ~ 10% of the collected light has > 20 reflections. This distorts the observed scintillator spectrum as discussed in Chapter 10. Since the reflections are dominantly diffuse, the light does not move very far along the 15.5 meter cell, doing a random walk with a reflected angle proportional to the cosine of the angle to the normal of the cell walls. The typical light path stays within about ± 10 cm of the track which created the light, and the path length of the light in the scintillator before capture is then about 40 cm for the typical 8 reflections (see Figure 10.4).

Measurement of the reflectivity within an extruded cell is difficult to obtain without destroying the integrity of the extrusion. Instead, the reflectivity of PVC extrusions is routinely measured on the outside surface for quality control purpose (sections 12.4.3.1 and 12.4.3.2) with a portable spectrophotometer. The surface quality of the outside of an extrusion is burnished by the vacuum sizing, resulting in a more glossy finish. This is different than the quality of inside surfaces. However, the measurements of extrusions that have been cut open to expose the webs show negligible difference between the reflectivity measured on an outside surface and reflectivity measured on a web.

12.5.2 Light Yield

The light yield is a measure of the amount of light transmitted by the WLS fiber to an APD photodetector. For purposes of normalization, light is produced by a minimum ionizing particle traversing the center of a PVC cell filled with standard NOνA liquid scintillator. In order to isolate and study the contribution of PVC reflectivity to light, a PVC extrusion is equipped with WLS fibers and filled with liquid scintillator. See Chapter 10, Section 10.3.1 . This type of setup has been used to show that N-27 (with 15% anatase TiO2) outperforms N-24 (same formula except with 15% rutile TiO2) by ~ 15%, as shown in Figure 12.22.

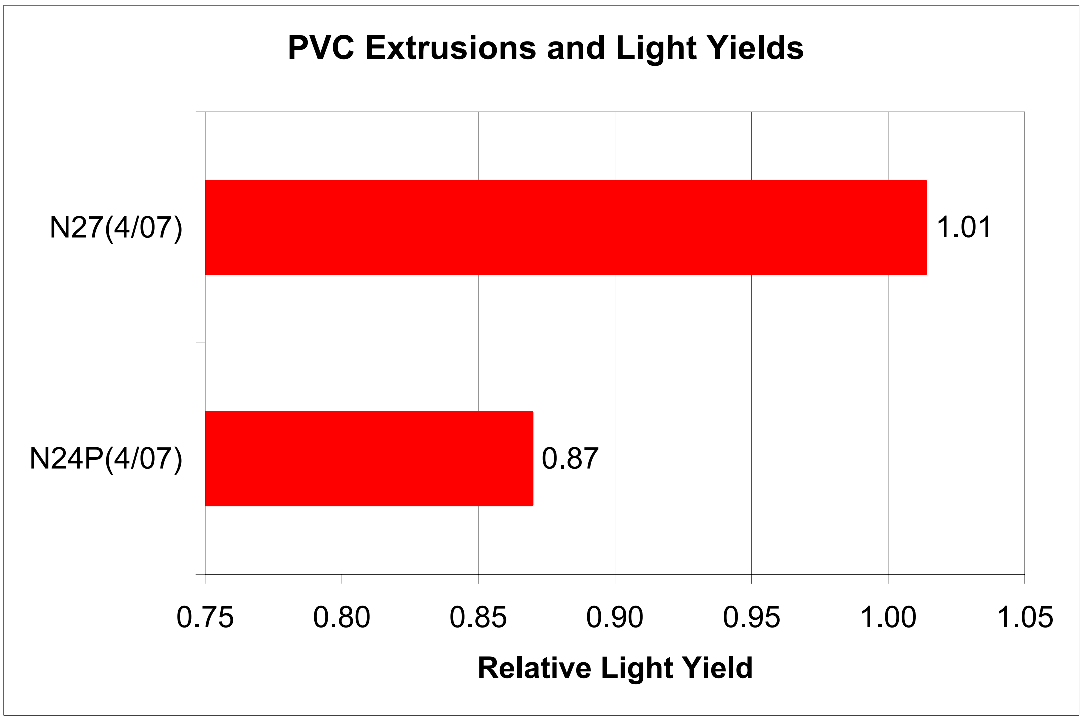

Fig 12.22: Light yields of N27 (15% anatase) compared to N24P (15%rutile).

12.6 Strength of the NOνA PVC Material

12.6.1 Introduction

In addition to containing the liquid scintillator and providing a surface with high reflectivity, the PVC extrusions form a self-supporting structure discussed in Chapter 17. The long term structural performance of the PVC is of primary importance. Analyzing and designing a suitable structure requires an understanding of specific mechanical properties. The situation is complicated by the fact that PVC is viscoelastic at room temperature. This implies that the material will effectively become less stiff over time and creep under a state of constant load. The most serious implication for the NOνA structure pertains to the structural stability, which is a function of stiffness. The reduction in stiffness over time creates the potential that a structure that is initially stable could be come unstable at some future time leading to catastrophic failure. To design against this situation with a quantifiable factor of safety, the time dependent creep modulus is needed at a time equal to expected lifetime of the structure. The design lifetime of the

NOvA structure is 20 years. Since it is not practical to wait 20 years to measure the creep modulus, this value is determined by predictive methods.

There are several methods for predicting long term creep. The methods vary between being partly based on theory, on the one hand, to being based on completely empirical relationships. These methods include elevated temperature tests that accelerate time as well as extrapolating "normal" room temperature data out to future time. It is recommended in [5] to seek agreement of at least two different predictive methods so that "... the designer can be reasonably certain" of the value. As an additional check, we look at the results in the context of the published data. While PVC properties depend on the formulation, comparison to other PVC compounds serves as an added set of bounds for the values found in our testing.

12.6.2 Mechanical Properties of Polymers[1]

To better understand the creep modulus, refer to Figure 12.23 to identify commonly used terms for describing the physical material properties. The figure shows a plot of the stress versus strain curve of a PVC material and is typical of a curve produced by a material that does not exhibit a well defined yield point (elastic limit). Ignoring time effects for the moment, assume that the blue curve in the figure is the instantaneous stress/strain curve of the material. In this sense, instantaneous refers to the time required to increase the stress in the material from zero to some particular value. Then at any particular stress, the strain is determined. At low stresses the response can be seen to be linear. The slope of the linear region is defined as the Modulus of Elasticity, *E* (Young's Modulus). The limit of elastic response is often associated with the linear region. Since the departure from linearity is a qualitative measure, it is engineering practice to use the so called "0.2% offset yield stress". This value is determined by constructing a line parallel to stress vs. strain curve (the black dash-dot line in Fig. 12.23), but shifting it along the strain axis to the point of 0.2% strain at zero stress. Then the (offset) yield stress, σ, is defined as that value of stress at the intersection of this shifted line and the stress/strain curve as shown in the figure.

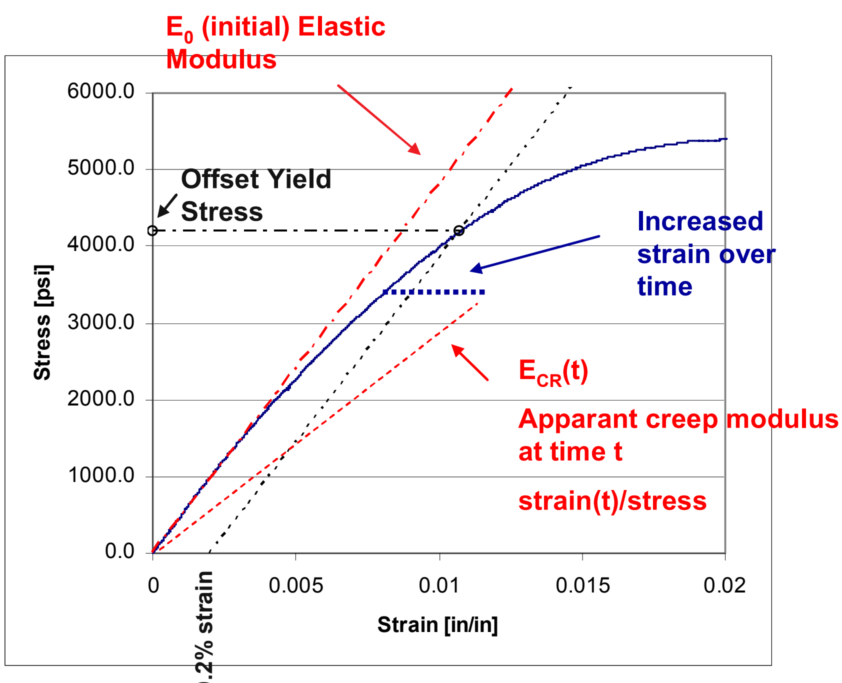

[1] References [6-8] apply to this entire section.

Fig. 12.23: Stress/ strain plot for a PVC material illustrating various values.

For linearly elastic materials below the yield stress, the strain of a material is related to the stress through Hooke's law, which for uniaxial stress is, $\sigma=E\varepsilon$ or $\varepsilon=\sigma/E$. For a material that does not creep, the modulus and therefore strain is constant over time as shown in the left plot of Fig. 12.24. This is not the case for a viscoelastic material such as PVC. When a constant load is applied, the material will have an instantaneous elastic deflection. However, as time increases with the loading remaining unchanged, the material will continue to deform so that the strain becomes a function of time as shown in the right plot of Figure 12.24. If we make a similar Hooke's law relationship noting that the stress remains constant, the creep modulus

$$E_{cr}(\sigma,t)=\frac{\sigma_o}{\varepsilon(t)}.$$

The term "apparent" creep modulus is often used here since the elastic modulus itself is not changing but is effectively becoming lower based on the increased strain with no change in stress. Because the FEA analysis solves for deflections based on applied stress, this relation between strain and stress is needed for calculations. Likewise, $E_{cr}(t)$ is determined by measuring $\varepsilon(t)$ in uniaxial test samples exposed to constant stress.

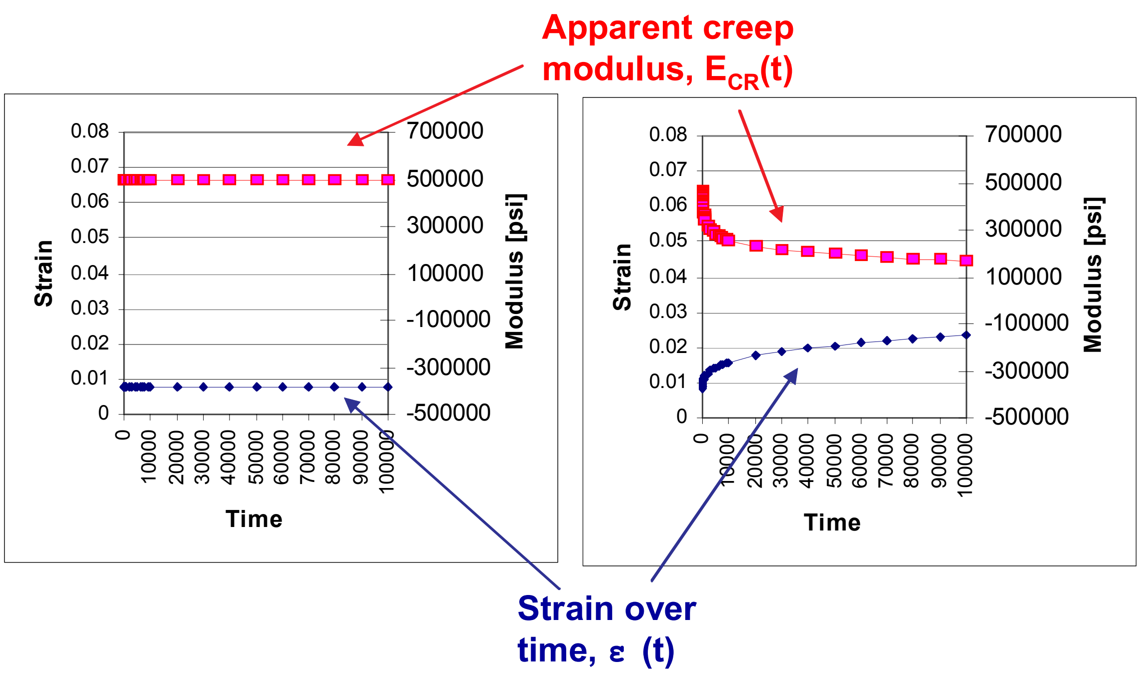

Fig. 12.24: Comparison plots of strain versus time (seconds) for a material under constant stress. The left plot shows strain ε(t) to be constant in time (zero creep) while the right plot shows strain as a function of time (creep). $E_{CR}(t)$ is the apparent creep modulus as discussed in the text.

It is helpful to think of the creep response as being made up of both elastic and viscous components. Figure 12.25 shows a simplified model using springs and dampers to represent these two components. A more accurate model would include an infinite series of springs and dampers that give rise to a spectrum of relaxation times for the material. Again referring to the right plot in Fig. 12.24 and noting the load is applied at *t=0*, one can see there is an immediate strain which comprises the elastic part of the response. As time increases, the material keeps moving in a viscous sense but with increasing resistance to flow. To emphasize this elastic component, it is noted that when the load is removed at any time, the strain is immediately reduced by the amount of the initial elastic strain. That is, the elastic strain is immediately recovered.

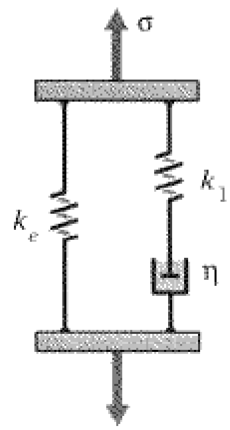

Fig.12.25: Zener model of a viscoelastic solid.

The definition of the creep modulus above included a stress dependence which is true for the general case and at large strains. When strains are small enough, less than 0.005, the creep modulus becomes independent of stress. This range of operation is defined as the linear viscoelastic (LVE) range. The NOνA structure is designed to limit stresses such that its mechanical creep properties are confined to the LVE range. This allows the use of linear analysis and it also allows for a variety of predictive methods. Additionally, the creep strains are fully recoverable in the (LVE) range. That is, given enough time upon load removal, the material will return to the initial state.

In the above, we specifically describe the situation of creep which is the increased strain over time of a material subject to constant stress. A counter example is to subject a material to a constant strain and then observe the stress. The stress would then reduce in time due to the process called stress relaxation. Both of these processes result from the same viscoelastic mechanisms.

An important characteristic of PVC and polymers is that mechanical properties are strongly dependent upon temperature. Properties such as the creep modulus need to be understood relative to the service temperature.

Before discussing the methods of determining the creep modulus and thee measured data, it is worth noting some PVC literature references. There are not material standards for PVC and published data for PVC creep is generally not available. This is likely due to the fact that the properties depend on the formulation. The NOνA formulation is generally like a PVC pipe resin except that the TiO_2 concentration is significantly higher but there are no additional fillers. Comparison of our results to PVC creep data in the literature is helpful for two reasons in spite of the fact that the PVC formulations are not identical. First, the available data can provide a bound on values as and it can indicate the typical shape of the curve. Second, since much of the data involves predictive methods it adds information on the accuracy of predictions.

A long term study of PVC creep over 26 years was done using stress levels of 2000 and 4000 psi at 24 ºC [4]. Using a relation $\varepsilon = \varepsilon^0 + \varepsilon^+ t^n$ to predict the creep where ε^0 and ε^+ are constants determined at after 1900 hours of data, the 26-year creep was over predicted to less than

5%. The 20 year creep modulus was measured at 156 ksi for a stress of 4000 psi. Some predicted data by a manufacturer for a range of his formulations showed values in the range 200 – 60ksi. The formulations with the lower values were identified as Ultra Flow and are likely injection molding compounds designed with lower viscosity and not representative of the NOvA material. With the exception of the PVC expressly formulated for injection molding, it is shown below that all estimates of NOVA PVC creep are below these values. That is, the NOVA estimates are not exceeding values found in literature.

12.6.3 Creep Tests and Predictions

As has been discussed elsewhere, the NOvA material has been specially formulated due to the unique requirements upon the mechanical and reflective properties as well the ability to extrude reliably in the complex NOvA die geometry. The final material choice is referred to as NOvA-27. Due to the long times needed in studying creep, creep studies were begun at various times using previous related formulations. The results of the tests with these other formulations are presented as a basis and support of the methods of evaluating creep. Studies of the NOvA-27 are in the early stages and will continue. The differences in the formulations relate mostly to small quantities of internal lubricants and are discussed further with the data below.

	Rutile			Anatase	
	PET-B	**Nova 2**	**Nova 24**	**Nova 23**	**Nova 27**
PVC	82%	77%	78%	75%	78%
Titanium Dioxide	15%			18%	15%
Lubricants/Stabilizers/ Processing aids	2.9%	4.2%	4.6%	4.5%	4.6%
Impact modifiers	0%	4%	3%	3%	

Table 12.2: Comparison of various NOVA formulations grouped by type of titanium dioxide (rutile/anatase) to show relative similarity of formulations . There is a variation in the amounts of lubricants and types of stabilizers. Significant variation of creep properties is not expected as PVC resin is identical in each case.

12.6.4 Methods of Determining the Long Term Creep Modulus

There are three common methods for predicting the long term creep modulus. These are:

1. Extrapolation of long term data- Power law prediction (Finley relation)
2. Time-Temperature Superposition (TTS)
3. Frequency-Time-Temperature-Superposition (FTTS)

The first method is used simply to extrapolate real time data. Generally, extrapolating from existing data is not recommended more than one order of magnitude beyond the last data point. One common formula used is the Finley relation, $\varepsilon(t) = \varepsilon^0 + \varepsilon^+ t^n$ where ε^0 and ε^+ are constants determined from the existing data. This method is based on a long term study and was used to accurately predict PVC creep past 20 years based on data obtained in the first 80 days [1]. These tests are normally done at the expected service temperature.

The second and third methods rely on a relationship between the time response and temperature of the material. Recall from above that a viscoelastic material can be thought to be a combination of springs and dashpots with different time constants. In the case of creep, these constants are referred to as the retardation times, which depend on the temperature. If a material is "thermorheologically simple", the retardation times at one temperature are linearly related to those at another temperature through a temperature dependent proportionality constant. By using the Zener model as a reference, this principle can be used to show a correlation between increasing temperature and a shift in the creep time curve. This forms the basis of the Time-Temperature superposition.

The idea behind the second method of predicting creep is to make a determination of the creep modulus at various temperatures in short times compared to the ultimately desired time. The curves at different temperatures are then shifted along the log time scale and assembled together to form a reference curve for the creep modulus over an extended time range at a single temperature.

The third method also counts on this temperature superposition but uses a different method for determining the creep at each temperature. It takes advantage of an additional relationship between time and frequency response of viscoelastic materials. If a viscoelastic material is subjected to a time varying stress, the corresponding strain will vary but with lagging phase compared to the applied stress. Using frequency transform techniques, the frequency response data can be directly transformed to the time domain. This method is very well documented [e.g.,6-8] and is the best method for determining the initial (short term) modulus. This results from the fact that during a normal tensile test the load is slowly increased while the strain is measured. However, the strain is dependent on the load history and the result from a tensile test will vary depending on the machine speed. That is, polymers are very rate sensitive. The frequency test solves this problem but suffers from limits such that it is not practical to try and measure at frequencies corresponding to the inverse of long times. To solve this, the test is carried out over the largest practical frequency range of the machine at various temperatures. The results are then transformed using the time-temperature superposition method described above.

All three techniques are utilized to characterize the NOvA material. We use the FTTS method as the basis of the long term prediction. We then use long-term data to check agreement over short time scales, with the eventual goal of having enough data to extrapolate one order of magnitude in time. We then make an additional prediction using the TTS method through elevated temperature tensile creep tests. In addition to this, we perform the long term and TTS test into completely different set-ups as a cross check. Our desire is to find general agreement among these different methods. As is shown below, all of this data supports the use of the so-called PET-B "worst case" estimate as a conservative lower bound on the creep modulus that is used in the FEA analysis.

12.6.5 Difficulties due to aging

Before discussing the results of the creep tests, it is important to briefly introduce the concept of physical aging which is referred to frequently below. The Time-Temperature superposition described above is rigorously valid above the glass transition temperature, T_g [17]. This is not the case below T_g where the effects of "physical aging" need to be considered. Physical aging is associated with the slow loss of excess free volume that remains in the material after quenching. The effect is described by the aging time, t_e, which is the elapsed between quenching and the time of load application [7]. It has been shown for PVC that increasing t_e by a factor of 10 decreases the creep rate by a factor of 10 and shifts curve along the time scale to the right [9,10]. To correct for aging effects, one must add a vertical shift to the data in addition to the (horizontal) time shift [7,17]. This issue is important in understanding and interpreting the real time creep curves in Section 12.6.7.

12.6.6 *Twenty Year Prediction of NOvA PVC Using FTTS*

Due to the specialized equipment and expertise needed, an external consultant and lab were utilized to obtain the long term creep modulus prediction. Predictions have been made for four different Nova materials, PET-B [17], Nova-2 (also referred to as N2) [18], Nova-23 or N23, and Nova-24 or N24[19] using the FTTS method described above. As shown in Table 12.2, the compounds are all made with the same base PVC resin. The crystalline type of TiO_2 (rutile or anatase) is different, but it is the same percentage (15%) except for Nova-23 (18%). There is some variation in the quantities of lubricants in the resin formulation, as well as in type of stabilizer and type/quantity of impact modifiers. Creep properties are primarily driven by the PVC resin which is identical in all cases, so similar results are expected. The predictions were made using the FTTS method described above.

The results of all of the predictions are shown in Figure 12.26. In all cases, the same sample of each formulation was used by repeating the test at various temperatures allowing time for recovery between tests. As a starting point, for the case of PET-B, the materials were tested using several methods and interpreted with different assumptions as described in [17].

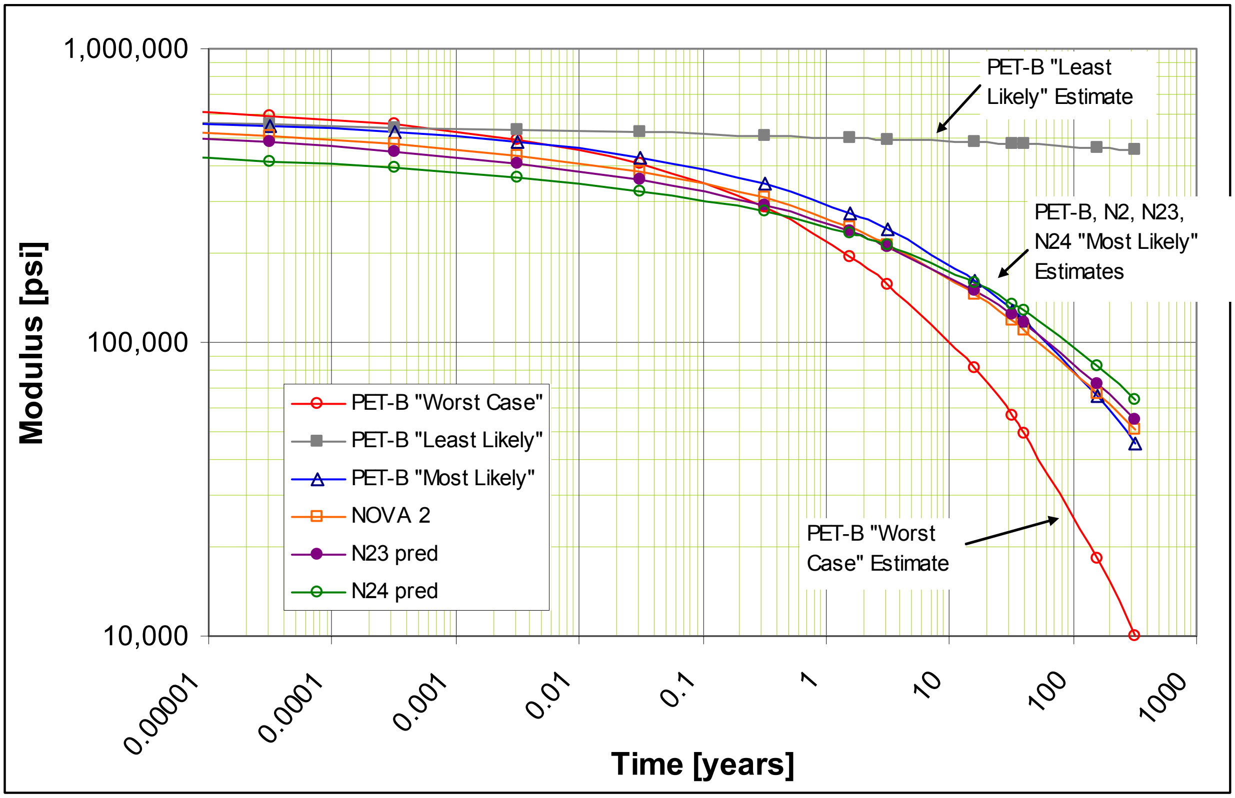

Fig. 12.26: Comparison of FTTS creep predictions. Original prediction was performed with the PET-B PVC formulation in three ways, or methods. The method labeled "Most Likely" is considered to give the best estimate. Therefore only this method is used in further tests. As is expected, the different formulations perform similarly when compared by same method.

The tests were performed on an early type of PVC called “PET-B”. Two types of tests were done; then an additional shift factor was added to each type. Type 1: start above T_g and decrease the temperature incrementally. Type 2: start at -20ºC and increase the temperature incrementally. The curve designated the "most likely" in Fig. 12.26 is taken from Type 1 tests, after adding the horizontal shift factor. The reason it is “most likely” is related to the physical aging, which has a tendency to reduce the excess free volume as the sample is slowly lowered from above T_g keeping the excess free volume in a near equilibrium condition.

Samples in the Type 2 tests have “increased motion”, or flow, due to the excess free volume that has yet to be removed. The curve designated “worst case” in Fig. 12.26 is from Type 2 tests, after adding the horizontal shift factor. Both the "worst case" and "most likely" curves also include a vertical shift factor that is not rigorously based but is recommended in the literature as a method to further account for aging effects. The curve labeled "least likely" in Fig. 12.26 is the result of Type1 tests but it does not include the vertical shift factor. It did not reflect any literature reference of real creep data and was therefore dismissed.

For the newer PVC formulations (NOVA-2, NOVA-23 and NOVA-24, also called N2, N23 and N24, respectively), the tests were performed and analyzed using only the "most likely” method. As can be seen in Figure 12.26, when comparing the creep curves for the four different formulations, PET-B, NOVA-2, NOVA -23, and NOVA -24, we see very similar performance. This is expected as the creep should be primarily driven by the PVC resin and all four formulations have the same PVC resin.

To be conservative, the FEA analyses presented in Chapter 17 were done using the PET-B "worst case" estimate.

12.6.7 Long Term Tests at 20 Deg C

To verify the “20-year predictions”, long term creep tests are being conducted at room temperature (without acceleration) in an effort to validate the values determined by the consultant. ASTM “dog-bone” samples made from the N27 formulation are placed in temperature controlled boxes maintained at 20ºC as shown in Figure12.27. These tests are run for much longer times than the accelerated tests, resulting in less extrapolation and adding confidence to the long term estimates.

Fig. 12.27: Long term creep samples instrumented with strain gages and kept inside a temperature controlled box at 20 deg C.

The real time creep data for the N27 material is compared to the accelerated creep estimates in Figure 12.28. Also the PET-B "worst case" curve is shown for reference as this is the curve used in the FEA in Chapter 17. In comparing the room temperature data with the estimate, the N27 data compares well after 116 days of testing.

In addition to the predicted value for the creep modulus, the consultant suggested a value of 730 psi for the limit of viscoelastic behavior (where creep modulus is independent of applied stress) based on current literature. The data in the test includes samples with stress ranging from 300-700 psi. The data for all three materials show no significant stress dependence and are consistent with the claim of linear viscoelastic behavior below 730 psi.

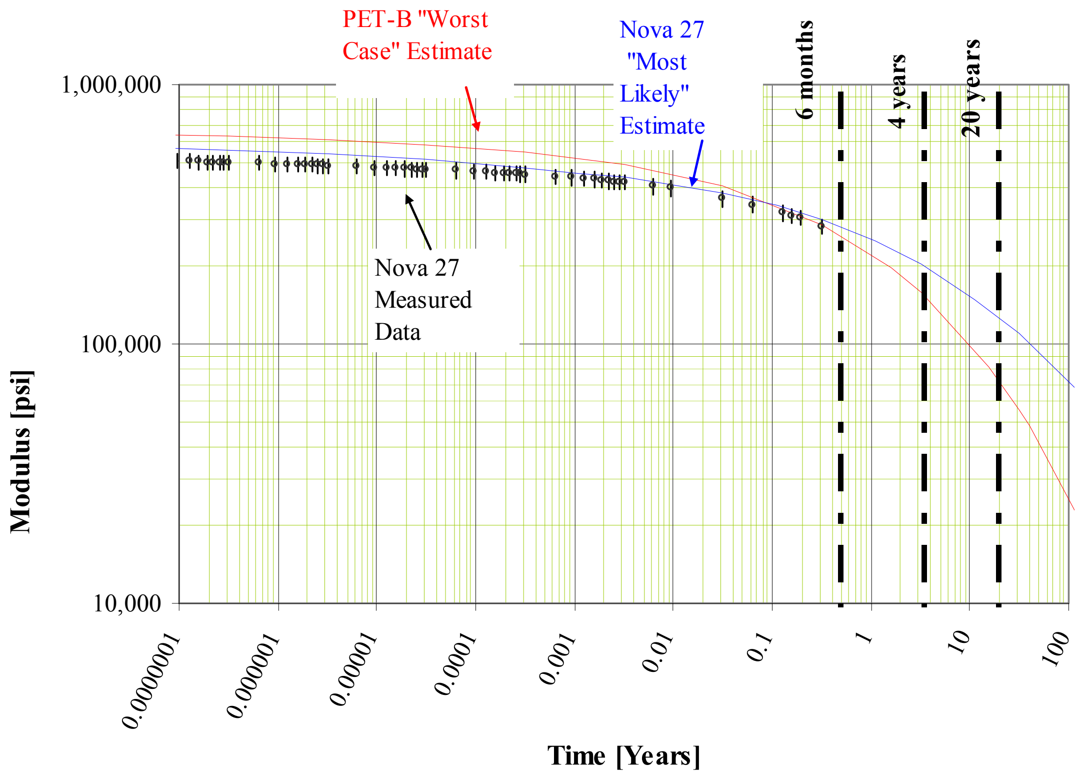

Fig. 12.28: Comparison of NOvA 27 room temperature creep data (black) creep modulus [psi] at 116 days to the consultant prediction for NOvA 27 (blue) "Most Likely Estimate" and PET-B (red) "Worst Case Estimate" material. The error bars represent a measurement uncertainty of 6%. The measured data is following the predicted curve.

12.6.8 Elevated Temperature Tensile Creep Tests

As an additional method of estimating the long term creep of the Nova formulations, tensile creep tests were performed on N2 samples at multiple temperatures. The results were then superimposed using “time-temperature superposition” method [20] to obtain an estimate of long time performance.

Figure 12.29 shows the three stations that reside inside a convection oven. The samples are placed under constant load using a hanging weight which is applied remotely via a cable support system. This allows load application after the samples are brought to temperature without requiring opening of the oven door. The strain is measured using extensometers that are attached to the samples. The extensometers are supported with a counterbalanced support system to prevent the addition of bending strains from the weight of the extensometer. This is shown in Fig. 12.30.

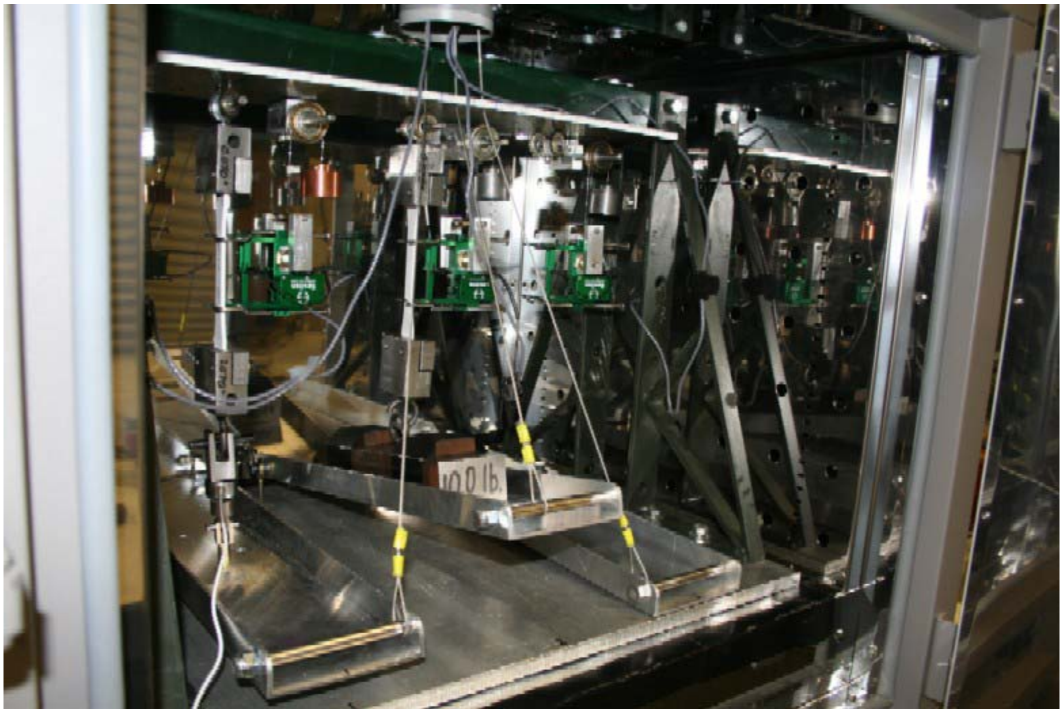

Fig.12.29: Three tensile creep stations located inside oven with remote load activation to allow accelerated creep tests at elevated temperatures. Extensometers are used to measure strain and are counterbalanced to prevent additional loading of samples.

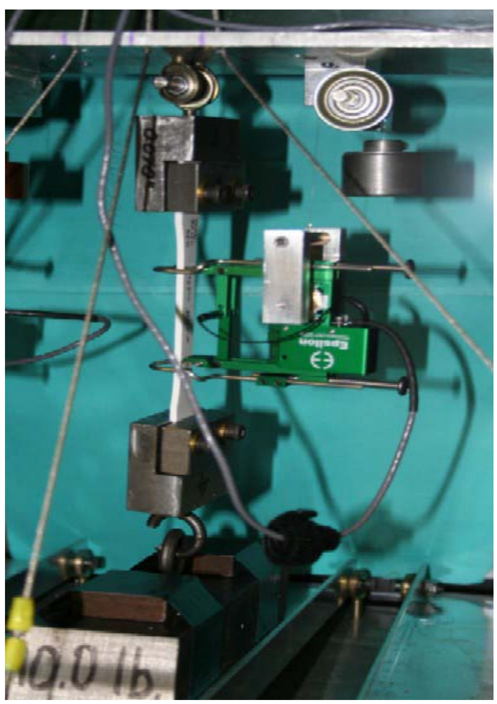

Fig. 12.30 Close-up view of sample mounting, counter balanced extensometer support, and remote activated load support. Cables can be seen to pass out the top of the fixture and out of a port in the oven.

The details of these tests are found in [20, 21]. Fig. 12.31 shows the N27 TTS prediction compared to the FTTS (frequency-time-temperature-superposition) predictions of both N27 and Pet-B ("worst case estimate") [9,10]. The plot shows N27 data obtained at 5 different temperatures (20, 40, 50, 60, and 70 deg C) . The 20 deg C temperature data is collected for 116 days and is plotted as large red circles on the plot to establish th reference temperature. The data obtained at higher temperature (and therefore accelerated in time compared to 20 deg C) are then shifted and superposed to extend the 20 deg data into future times. Due the physical aging of PVC (see 12.6.5) that results during the elevated temperature tests, the curves are shifted vertically along the modulus axis as well as horizontally along the time axis.

The plots show an apparent divergence in longer times. A more careful view would show that each set of data exhibits an upward change in slope of the modulus as the test time gets longer. This is a stiffness increase that is expected due to the physical aging. These tails are ignored when interpreting the results. When these tails are ignored, the shifted curves tend to follow the PET-B "worst case estimate" which is used in the FEA analysis as a conservative lower bound.

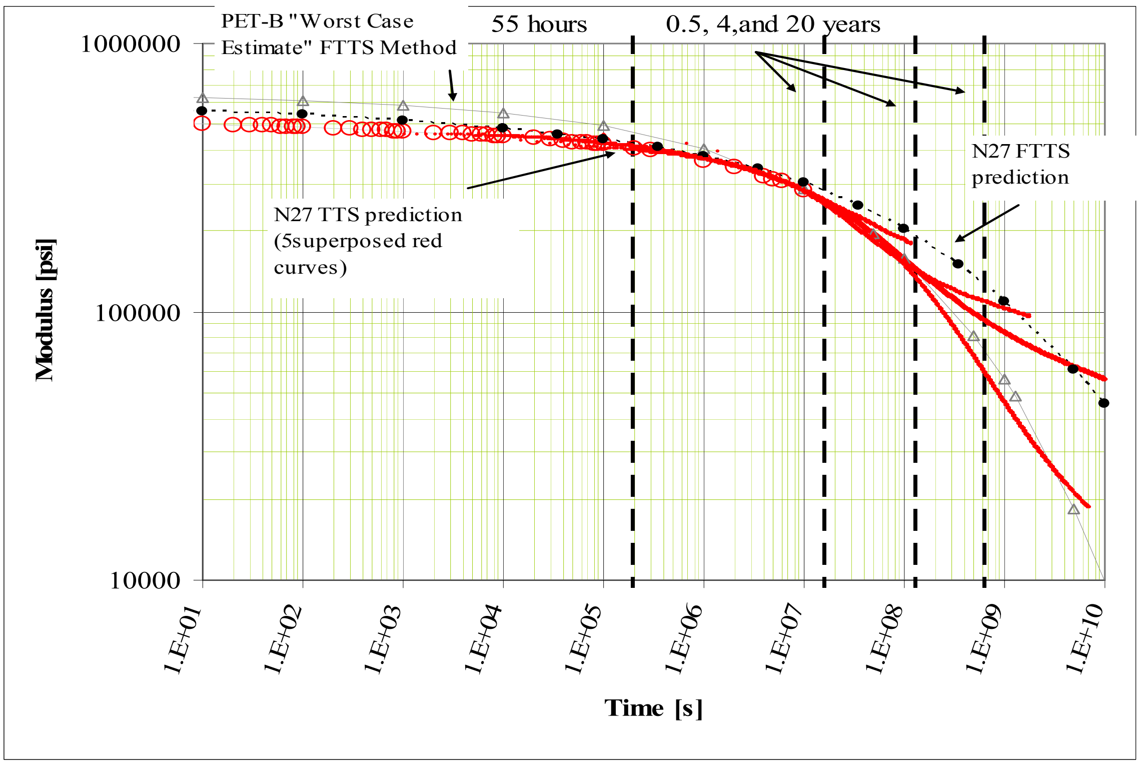

Fig. 12.31: Nova 27 master curve at 20 deg C as developed by accelerated temperature tensile creep tests (TTS) compared to Nova 27 (FTTS) master curve and PET-B (FTTS) "Worst Case" estimates developed by FTTS methods. The large red circles indicate the extent of data taken at 20 deg (non-accelerated).

The similarity of master curves obtained from these accelerated tensile creep tests and those developed based on the FTTS is interesting. While both methods rely on time-temperature superposition, the data were generated in completely different methods and over significantly different time scales. FTTS tests were done using dynamic techniques for short time periods (less than 5 minutes). The dynamic method makes a more accurate modulus measurement and the short time decreases the effects of physical aging on the tests. The downside is that the master curve is made with extrapolation of many orders of magnitude. The tensile creep tests described above are done on much longer time scale requiring significantly less extrapolation but potentially suffer from physical aging effects during the data taking, particularly in the longer times at higher temperatures. Measuring the short term modulus is also more difficult.

12.6.9 PVC Expansion due to Temperature and Humidity Changes

The thermal expansion coefficient for N27 PVC was determined by measuring the induced strain during a temperature change from 22to 60 deg C. The value was measured to be 6.0×10^{-5} in/in deg C. This value is consistent with published values of standard PVC.

Related to the thermal expansion, a test was conducted to evaluate the induced strain resulting from a humidity change. The details of this test are described in [22]. The change in strain was measured uisng a standard PVC dogbone specimen that was cut in the extrusion direction. The instrumented sample was initially at a temperature of 20.4 deg C at 57% RH (relative humidity). The humidity was raised to 92% and the corresponding strain measured. The time constant is slow and the induced strain occurs over weeks. After 512 hours, the sample strained 2.9×10^{-4} in/in. Dividing this value by the change in relative humidity gives a value of 8.6×10^{-6}. This value is approximately $1/7^{th}$ that of the thermal coefficient of expansion.

12.6.10 Impact Strength of NOVA compounds

PVC compounds exhibit less ductility than standard structural materials such as steel. Similarly, PVC can fail in a brittle manner due to unstable crack propagation. As brittleness and low ductility tend to be related, it is common to measure impact resistance. A common method of characterizing the impact properties of PVC is to use the Gardner Drop Dart Impact Test due to it's simplicity. This test consists of dropping a weighted "dart" from various heights upon the material samples to make a determination of the energy absorbing capability of the material. In our tests, the weight is 8 lbs. The dart is a steel cylinder where the tip is ½" diameter and the impacting point is rounded to a full radius. The test procedure is defined in [25] and the results of various impact tests performed on the NOvA materials are detailed in [26].

The impact tests gives information about the energy absorbing ability of the structure. The test depends on the geometry of the test specimen as well as the material. Therefore it is not a true material property and only provides relative comparison. In general, the tests have considerable scatter and at best general trends are sought. Figures 12.32 and 12.33 show impact results from two different materials to illustrate a relative comparison. Figure 12.31 shows the results of impact test performed on both vertical and horizontal extrusions made from the NOvA 27 PVC formulation. The vertical extrusions have a wall thickness that is 1.5 times thicker than that of the horizontals. Figure 12.32 shows a comparison of extrusions made from NOvA 24 material (a previous version using rutile TiO2). The Nova 24 material has similar thickness as the N27 horizontal extrusions.

A few observations can be made from these tests. First, there is a tendency for the outside cells to absorb more impact energy and this is likely based on geometry. The trend is more apparent in the N24 samples but has been seen consistently in most testing. Comparing the impact values between the two materials, the values are generally much lower for the N27 material indicating a more brittle behavior than the N24 material. The data shows relatively low impact strength for the formulations and also shows no apparent improvement with increased thickness. Visual inspection of the impact patterns of the N27 material show some marginal ductility prior to fracturing in a brittle fashion. In comparison, the N24 samples show significantly more ductility. This is consistent with elongation measured in tensile tests of N27 which was typically about 20% compared to 50% of the other NOvA formulations [27].

To understand the effects of time on impact properties, an impact sample was heated at 60 deg C. Figure 12.33 shows the results of impact test performed on aged and un-aged samples of NOvA 24. Aged samples were heated at 60 deg C for 19 hours. A small reduction in impact energy is observed.

It is not possible to use the impact energy information gathered from dart tests for design. Fracture mechanics tests are necessary to produce the design values. These tests are planned for the N27 materials to help quantify the fracture toughness better.

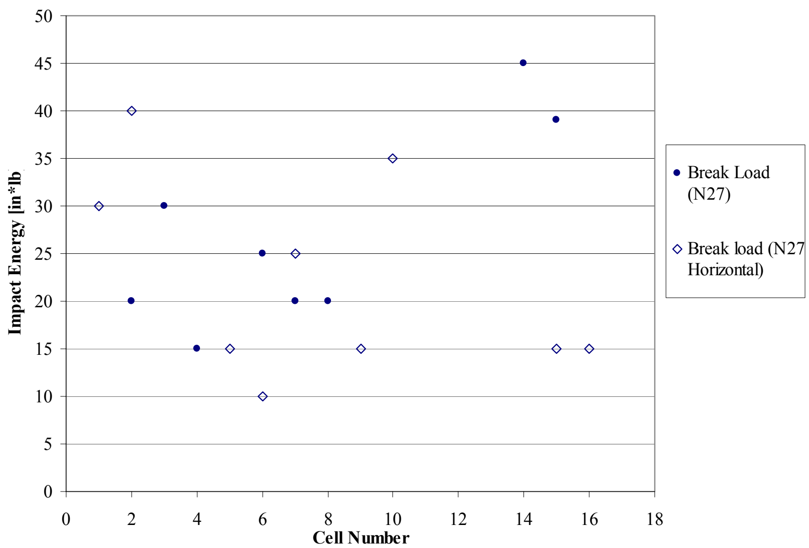

Fig. 12.32: Impact test results for vertical and horizontal extrusions made from NOvA 27 PVC material.

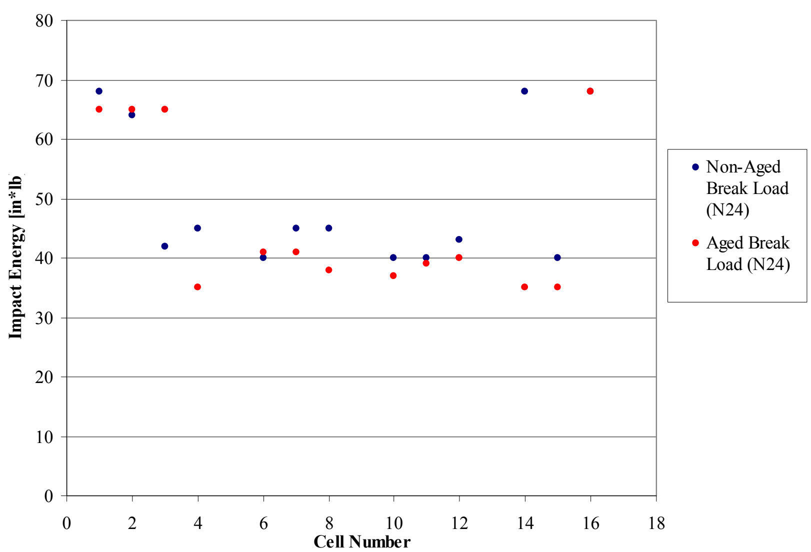

Fig. 12.33: Impact energy comparison between aged and un-aged NOvA 24 PVC extrusions. Aged samples were heated at 60 deg C for 19 hours. A small reduction in impact energy is observed.

12.6.11 PVC Scintillator exposure

Polymers can become brittle from exposure to certain liquids. PVC normally has good resistance to many liquids but there is no information available on exposure to liquid scintillator. Several methods have been used to find any sign of adverse effect resulting from liquid scintillator contact. These are described further in [23].

A first simple test was performed in which samples of the PVC were immersed in liquid scintillator and then the weight before and after soaking of the samples was compared. The samples were soaked at room temperature for 1, 2, 7, and 30 days and were measured on a high precision scale. No observable change was detected.

In order to evaluate the mechanical properties, PVC dog-bone tensile test specimens were soaked in liquid scintillator for as long as 12 months. These samples were removed and the tensile properties were measured. The properties were then compared to identical samples that were stored in open air next to the soaking samples for the same time period. No difference in the ultimate strength not total elongation was observed.

The results of the above tests do not indicate any potential adverse effect on the PVC due to interaction with the liquid scintillator. Continued tests are in progress to confirm this. These tests include large deflection bend samples immersed in liquid scintillator and slow strain tensile tests.

Figure 12.34 shows the large deflection bend and immersed in liquid scintillator. An identical set of samples is placed in air along side the soaked samples. The intent of these tests is to investigate any differences such as crack formation between the soaked and air samples. These tests are in progress.

The slow strain tests involve performing tensile tests wherein the test duration is several weeks. These tests, which are not yet underway, will be performed with soaked and un-soaked samples and the results of tensile measurements will be compared.

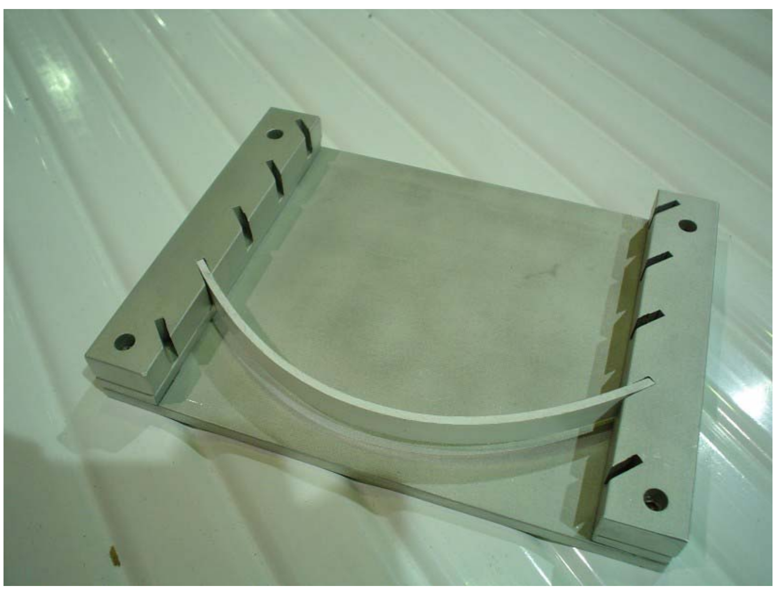

Fig. 12.34: Fixture for exposing greatly bent PVC samples to liquid scintillator.

12.7 Shipping and Handling

After PVC extrusions are cut to length on the production line, they are sorted, stacked and made ready for eventual shipment. The details of the sorting and stacking process, packaging, short-term storage, loading and shipping are presented below.

12.7.1 Sorting and Stacking

Extrusions are removed from the production line with a vacuum lifting device (Fig. 12.35) and placed onto one of four nearby shipping stacks with a wide-span gantry crane. As explained in Chapter 12.4.2, sorting is done on the basis of extrusion height. Each shipping stack consists of 8 equally-spaced pallets with bridge material of the same length as the extrusions tied to each pallet. Bridge material provides support for the stack of extrusions, as shown in Fig. 12.36. Once a stack is fully loaded, 30 extrusions high and two across (for a total of 60 extrusions), it is moved away and packaged for shipment.

Fig. 12.35: Photograph of the vacuum lifting device placing a prototype 52 foot-long extrusion on a shipping stack at the extruding factory. The vacuum suction cups, positioned with reference to the extrusion's edge, accommodate the scalloped outer surface. Note that the shipping stack has two extrusions, side by side. The red and yellow hoses supply air to the air caster system (refer to section 12.7.4).

Far Detector extrusions (51' 0" in length) are stacked 30 layers high (6' 8" in height) and 2 extrusions wide (4' 3" wide) on 8 evenly spaced commercial plastic pallets. An ablative pair of full length extrusions will form the support for the 60 extrusions, to be used to manufacture 30 modules, in order to facilitate loading and unloading without stressing any of the detector PVC (see Figure 12.36).

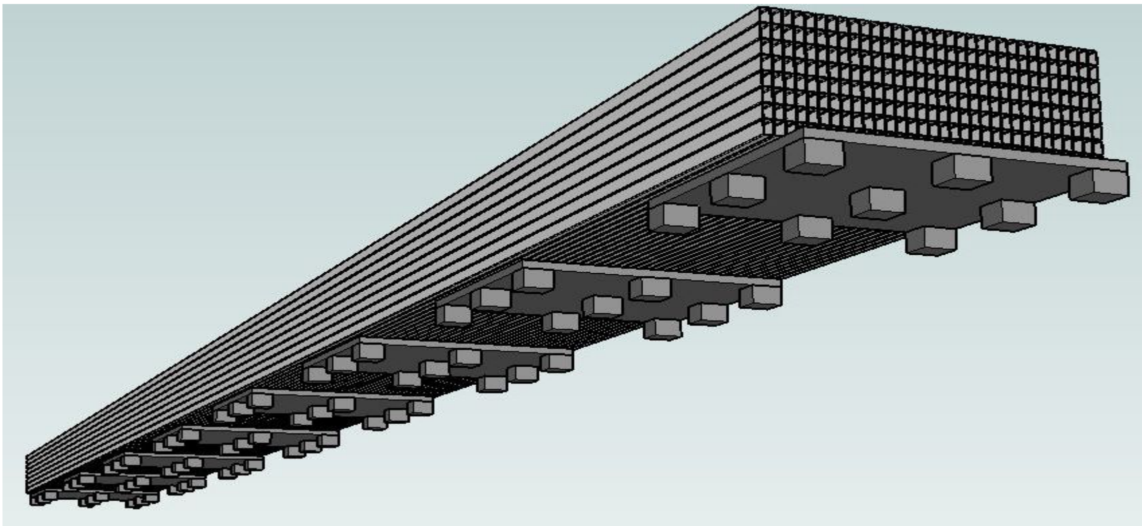

Fig. 12.36: Diagram of a partially loaded pallet system for Far Detector extrusion transportation. On the bottom are 8 industry standard plastic pallets. The first layer of material above the pallets consists of two side-by-side 16 cell extrusions that provide an ablative buffer against which the air lifter housings will press.

Seven pallets can support the stack load; but stress calculations indicate the maximum desired unsupported length between any two pallets requires eight. Plastic pallets were chosen because they can be nested together, aiding in transport and storage costs; they are supplied with a dynamic load rating sufficient for supporting the extrusions; and at 22 to 29 lbs each they are relatively light weight to handle (see Figure 12.37).

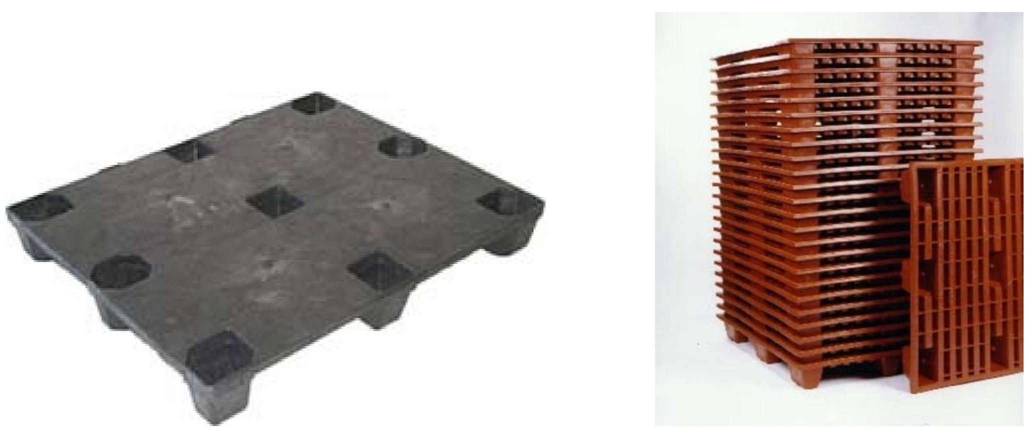

Fig. 12.37: Individual pallets are "nestable" for delivery to and storage at the extrusion facility. The dynamic load rating of each selected pallet is 5000 lbs.

The decision to use ablative extrusions as "bridges" between pallets for the support material is based on the ability to match the width of extrusions and modules precisely, and the efficiency of space and time such a choice will provide at the extrusion facility. The pallets and ablative extrusions will add < 9" to the stack height, leaving ~ 1' 5" for height clearance. The load must be centered in the transport trailer, leaving ~ 23.5" clearance on each side of the load. The ablative extrusions will be banded independently to the pallets with commercially available banding material. The open end of the extrusions will be wrapped in low tack polyethylene material and then the full stack will be banded using the same Tenax polyester strapping. A standard transport system of edge softeners and stiff stringers across the top of the stack will be employed to prevent crushing of the extrusions during banding.

12.7.2 Storage

In addition to 8 partially-filled stacks of sorted extrusions (4 thin-wall and 4 thick-wall), space is allotted for 24 full stacks of extrusions to be stored at the extruding company. The average population is 12 thin-wall (horizontal) extrusions and 12 thick-wall (vertical) extrusions. Production of horizontal extrusions will proceed for a period of 13 days before switching to production of vertical extrusions for 18 days. However, shipments to the module assembly factory have to toggle between horizontal and vertical stacks on an almost daily basis. For example, during horizontal production horizontal stacks are shipped every other day and vertical stacks, taken from storage, are shipped on the alternate days. On those days, horizontal stacks are placed into storage in order to have an adequate supply during vertical production. Stacks will be cycled through storage on a first in first out basis, so that no stack stagnates in storage for a long period of time.

12.7.3 Shipping

Candidate vendors for producing NOvA 16 cell extrusions are all located in the Midwestern U.S. The extrusions will be shipped to the Module Factory (see Chapter 13) by enclosed "dry van" trucks. The Far Detector extrusion lengths are sized such that finished modules will be transportable inside the 52' 5" length x 8' 10" height x 8' 2" width envelope of a standard semi-trailer (see Figure 12.38). The weight of a stack of the heavier, vertical extrusions will be ~ 30,000 lbs. Normal over the road net weight limits for 53' semi tractor-trailer trucks is 45,000 lbs.

Fig. 12.38: Diagram of Far Detector extrusion stack envelope inside a standard 53' semi-trailer. Enough space from front to back has been maintained for slight off-axis loading, as well as packing material.

Transportation of the ~24,000 extrusions requires 422 truckloads and about 3,376 pallets in addition to the 2 extra extrusions for every 60 destined to be assembled into modules. Recycling the pallets and ablative extrusions after they have completed the journey to the assembly site reduces these numbers to 1,624 pallets and 348 ablative extrusions. This includes the extrusion totals for the Far Detector; spare pallets and ablative bridges are included.

12.7.4 Motion System

A system of air casters (see Figure 12.39) is used to move the ~ 30,000 lb. (max.) stacks on and off the trucks, as well as around the factory floors. Height required for air lifting is less than 1". Overlay mats designed for loading docks and truck beds will be employed to ensure smooth operation of the air casters over uneven surfaces. Air casters will not travel with the load; and must be able to be removed and inserted in the space between the side of the trailer and the load. Ease of control of motion and lack of wear on parts and flooring make the air system the best alternative for maneuvering the 522 stacks of Far Detector extrusions from the extrusion facility to the Module Factory location. Additionally, the system has been designed to carry through to the Far Detector site utilizing the same scheme of pallets, bridges, banding and air motion. Then the pallets and ablative extrusions are cycled back to the factory and to the extruding vendor.

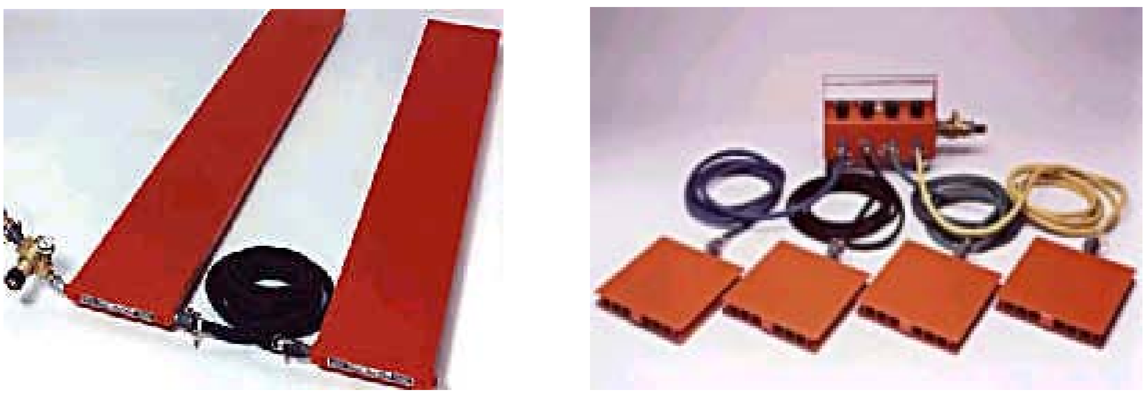

Fig. 12.39 Illustrations of standard air plank or air caster systems used for moving the extrusion loads. Custom sizing will provide the correct footprint for the space between pallets as well as the overall load weight of 30,000 lbs for the heaviest vertical extrusion loads.

12.7.5 Prototype Extrusions, Stacking and the Motion System

A verification of the stacking procedure, packaging and motion system was performed with vertical prototype extrusions. A foundation for the stack was assembled with plastic pallets and bridge extrusions tied to the pallets. Vertical prototype extrusions were stacked to a height of 25 extrusions (two extrusions wide), packaged and moved into a truck via an air caster system. A representative from the air caster company was present to demonstrate the system and assist with its operation. Figure 12.40 show the pallets and bridge extrusions tied to them The vacuum lifting fixture and gantry were used to load vertical extrusions onto the bridges, forming the beginning of a stack.. Air casters are in between the pallets, powered by pressurized air.

Figure 12.41 shows a photo of the loaded stack just prior to pressurizing the air casters to move it into a truck at the loading dock of the extruding company. Cracks in the floor were sealed with tape and a plastic tarp was extended into the truck to to provide a smooth surface for the air casters to function properly. This is shown in Fig. 12.42.

The procedure of loading a stack of extrusions into the truck (Fig. 12.43) took only a few minutes. The stack was then unloaded using the same methods.

Fig. 12.40: Photograph of the prototype stack foundation, consisting of plastic pallets and ablative or "bridge" extrusions tied to the pallets. The first layer of extrusions is being lifted onto the stack by means of the vacuum lifting fixture. Air casters are the red objects beneath the bridge extrusions. Note the black ties between pallets and bridge extrusions.

Fig. 12.41: Photograph of the stack, packaged by strapping tape over cardboard to protect the extrusions. No plastic covers were used because this load was used to demonstrate the motion system and was not shipped at that time.

Fig. 12.42: Photograph of the tarp used to provide a smooth surface from the factory floor into a truck at the loading dock.

Fig. 12.43 Photograph of the stack, weighing 25,000 lbs, being nudged into the truck with a forklift.

12.8 Changes in the PVC Extrusion Design Since the CDR

The changes since the CDR are

- reduced width of extrusion from 32 to 16 cells
- changed to anatase TiO_2 instead of rutile
- eliminated the edge stiffeners because they will no longer be extruded. (Instead they will be purchased and cut to size, and are now discussed in Ch. 13.)
- slightly smaller extruded cell widths to assemble a plane of modules to the proper size
- shorter extrusion lengths to allow an extrusion module to fit into a closed truck

12.9 Work Remaining to Complete the Extrusion Design

Confirm that N-27 will be a suitable resin for producing vertical extrusions of the proper size, strength and reflectivity. Residence time of the resin will be longer in the vertical die, which requires good stability against sticking or burning in the die. Longer residence time is caused by slower flow due to the vertical extrusion's thicker walls and webs. Tests with the prototype vertical extrusion die are now in progress.

12.10 Chapter 12 References

[1] See for example "Polymers, Light and the Science of TiO2", DuPont Technical Liabraries, 2002 (available at the SpecialChem website), or similar publications by Millenium Chemicals and other titanium dioxide suppliers.
[2] K. Ruddick, NOνA docdb note # 211, December, 2005.
[3] C. Bower, NOνA docdb note #208
[4] Findley, W.M., "26-Year Creep and Recovery of Poly(Vinyl Chloride) and Polyethylene", Polymer Engineering and Science, Vol. 27, No. 8, pp. 582-585, 1987.
[5] *Engineering Material Handbook, Volume 2: Engineering Plastics*, ASM International, 1985.
[6] McCrum, N.G., Buckley, C.P., and Bucknall, C.B., *Principles of Polymer Engineering*, Oxford Science Publications, 1997.
[7] Gibson, R.F., *Principles of Composite Materials*, McGraw Hill, 1994.
[8] Krishnamachari, S.I., *Applied Stress Analysis of Plastics: A Mechanical Engineering Approach*, Van Nostrand Reinhold, 1993.
[9] Brostow, W. and Corneliussen, R.D., *Failure of Plastics*, Hanser, 1986.
[10] Struik, L.C.E., "The Mechanical Enhancement of Physical Aging", Polymer, Vol. 21, August 1980, pp. 962-7.
[11] Teoh, S.H., "Predicting the Life and Design Stresses of Medical PLastics Under Creep Conditions", Biomaterials' Mechanical Properties, ASTM STP 1173, ASTM, 1994, pp. 77-86.
[12] Brueller, O.S., "On the non-linear characterization of long term behavior of polymeric materials", Polymer Engineering and Science, Vol. 27, No. 2, pp. 144-8, 1987.
[13] Lee, H.H.D., McGarry,F.J., "A creep apparatus to explore the quenching and aging phenomena of PVC films:, Journal of Materials Science, Vol. 26, 1991, pp.1-5.
[14] Read, B.E., Dean, G.D., and Tomlins, P.E., "Creep and physical aging of pVC: dependence on stress and temperature", Journal of Non-Crystalline Solids, 1994, pp. 562-8.
[15]Gaube, E., Diedrich, G., Muller, W., "Thermoplastic Pipes: Experience of 20 years Creep rupture testing", (translated from Kunststoffe, Hanser Verlag, vol. 66, No.1, January 1976, p1-4).
[16] Gang, X., "Linear extrapolation for prediction of tensile creep compliance of polyvinyl chloride", Journal of Harbin Institute of Technology, Vol. 12, No.5, 2005.
[17] Harrell, E.R.,"Modeling of the Creep Modulus of PVC 1111-BB [PET-B] for predicting creep at 20ºC for 20 years", NOνA DocDB 667, March 3, 2006.

[18] Harrell, E.R.,"Modeling of the Creep Modulus of NOvA 2P for predicting creep at 20ºC for 20 years", NOvA DocDB 1042, July 25, 2006.
[19] Harrell, E.R.," Modeling of the Creep Modulus of N23 and N24 for predicting creep at 20ºC for 20 years Creep", NOvA DocDB 1326, January 1,2007.
[20] Grudzinski, J.J, "NOVA 2 Creep Master Curve at 20 deg C as Determined from Elevated Temperature Tensile Creep Tests", NOvA DocDB 1976, May 16, 2007.
[21] Grudzinski, J.J, "NOVA 27 Creep Master Curve at 20 deg C as Determined from Elevated Temperature Tensile Creep Tests", NOvA DocDB 2677, October 2, 2007.
[22] Grudzinski, J.J, "Expansion due to humidity changes in PVC", DocDB 1535, March 15, 2007.
[23] Grudzinski, J.J, " Investigation of effects of liquid scintillator on NOVA PVC compounds", NOvA DocDB 2676, October 2, 2007.
[24] Perry's Chemical Engineer's Handbook, 6th edition,1984.
[25] Grudzinski, J.J, " Procedure for measuring relative impact strength of NOVA extrusions using the Drop Dart test", NOvA DocDB 2661, November 21, 2006.
[26] Grudzinski, J.J, " Impact strength tests of NOVA extrusions using the Drop Dart test", NOvA DocDB 2675, October 2, 2007.
[27] Grudzinski, J.J, " Tensile Properties of NOVA compounds", NOvA DocDB 2674, October 2, 2007.